Journal of Computational Science 53 (2021) 101368

Contents lists available at ScienceDirect

Journal of Computational Science

journal homepage: www.elsevier.com/locate/jocs

Evolutionary Rao algorithm☆

Suyanto *, Agung Toto Wibowo, Said Al Faraby, Siti Saadah, Rita Rismala

School of Computing, Telkom University, Bandung, Indonesia

ARTICLE INFO

Keywords:
Evolutionary Rao algorithm
Exploitation-exploration balance
Fitness-based adaptation scheme
Random walk
Two subpopulations

ABSTRACT

This paper proposes an evolutionary Rao algorithm (ERA) to enhance three state-of-the-art metaheuristic Rao algorithms (Rao-1, Rao-2, Rao-3) by introducing two new schemes. Firstly, the population is split into two sub-populations based on their qualities: high and low, with a particular portion. The high-quality sub-population searches for an optimum solution in an exploitative manner using a movement scheme used in the Rao-3 algorithm. Meanwhile, the low-quality one does in an explorative fashion using a new random walk. Secondly, two evolutionary operators: crossover and mutation, are incorporated to provide both exploitation and exploration strategies. A fitness-based adaptation is introduced to dynamically tune the three parameters: the portion of high-quality individuals, mutation radius, and mutation rate throughout the evolution, based on the improvement of best-so-far fitness. In contrast, the crossover is implemented using a standard random scheme. Comprehensive examinations using 38 benchmarks: twenty-three classic functions, ten CEC-C06 2019 benchmarks, and five global trajectory optimization problems show that the proposed ERA generally outperforms the four competitors: Rao-1, Rao-2, Rao-3, and firefly algorithm with courtship learning (FA-CL). Detailed investigations indicate that both proposed schemes work very well to make ERA evolves in an exploitative manner, which is created by a high portion of high-quality individuals and the crossover operator, and avoids being trapped on the local optimum solutions in an explorative manner, which is generated by a high portion of low-quality individuals and the mutation operator. Finally, the adaptation scheme effectively controls the exploitation-exploration balance by dynamically tuning the portion, mutation radius, and mutation rate throughout the evolution process.

1. Introduction

The metaheuristic optimization algorithms can be categorized into two groups: evolutionary algorithms (EAs) and swarm intelligence (SI) algorithms [1]. EAs are inspired by both evolution and natural selection, such as Genetic Algorithm (GA) [2], [3], Evolution Strategies (ES) [4], [5], and Differential Evolution (DE) [6]. Meanwhile, SI algorithms are inspired by a natural swarm, such as Particle Swarm Optimization (PSO) [7], [8], Firefly Algorithm (FA) [9], [10], Grey Wolf Optimizer (GWO) [11], [12], and Ant Lion Optimization (ALO) [13].

GA is one of the most popular EAs introduced in the 1970s [14]. It uses both evolution and natural selection that are applied to its population over generations. A population consists of some individual chromosomes, each representing a candidate solution. The new chromosomes in a generation are either some of the best chromosomes (elitism) in the previous generation or generated by genetic operations, such as crossover and mutation. The crossover takes two chromosomes and produces one offspring inherited part of chromosome values from each parent. In contrast, the mutation is randomly changing some values in a chromosome. The mutation is responsible for exploration, while crossover and elitism direct toward exploitation. GA can avoid being trapped in the local optima. It is also applicable to non-differentiable and high dimensionality functions. On the other hand, it converges slowly because of the highly-random operations that do not give a clear direction to find the global optimum solution quickly. However, various improvement schemes have been proposed to overcome the drawback, such as a concept of human-like constrained-mating [15] that creates a more explorative search strategy.

In 1995, the Particle Swarm Optimisation (PSO) was introduced by Kennedy and Elberhart [16]. The movements of the particles in searching for a global optimum mimics the behavior of bird flocking and fish schooling. PSO is one of the most popular SI algorithms since it has three

☆ This research is funded by the Directorate of Research and Community Service or *Direktorat Penelitian dan Pengabdian Masyarakat* (PPM), Telkom University, with grant number: 444/PNLT3/PPM/2020.

* Corresponding author.
E-mail addresses: suyanto@telkomuniversity.ac.id (S. Suyanto), agungtoto@telkomuniversity.ac.id (A.T. Wibowo), saidalfaraby@telkomuniversity.ac.id (S.A. Faraby), sitisaadah@telkomuniversity.ac.id (S. Saadah), ritaris@telkomuniversity.ac.id (R. Rismala).

https://doi.org/10.1016/j.jocs.2021.101368
Received 4 January 2021; Received in revised form 12 March 2021; Accepted 4 April 2021
Available online 9 April 2021

advantages: easy to implement, few parameters that are simply tuned, and effective in searching the global optimum solution since it has a clearer direction than GA. However, it tends to prematurely converge on a local optimum in optimizing a multimodal function since it uses a static finite leader and group based on a linear movement. Therefore, some strategies are developed to tackle the issue, such as a learning structure [17] to decouple exploration and exploitation and a dynamic updating of the inertia weights [18] to control the convergence.

In 2009, the Firefly Algorithm (FA) was proposed [19]. In FA, each firefly will be attracted to all other brighter (better) fireflies, not only to the global best like in PSO. Also, the brighter firefly's attractiveness is decreased proportioned to the distance between the two fireflies due to the light absorption. Since the fireflies will usually be attracted more to their brighter neighbor than the further away brightest individual, the exploration is more effective than PSO. In other words, FA uses a dynamic leader and group based on a nonlinear movement. Moreover, FA can be turned into PSO by setting the light absorption parameter such that every firefly can be seen clearly by all other fireflies. Consequently, all fireflies will be attracted to the brightest one (global best). In some experiments, FA shows better performance than PSO due to two critical characteristics [20]: 1) FA usually divides its population into a subgroup, 2) By not having an explicit global best, FA can avoid premature convergence. Several improved schemes are created to enhance the FA performance, such as a courtship learning framework [21], where the population is divided into subpopulations: female and male, to improve the convergence speed and solution accuracy. Another improvement scheme is the best neighbor guided strategy [22], where each firefly is attracted to the best firefly among some randomly chosen neighbors to decrease the firefly oscillations in every attraction-induced migration stage as well as increase the probability of the guidance a new better direction.

In 2014, Grey Wolf Optimization (GWO) was introduced by Mirjalili [23]. It is inspired by both the social hierarchy and hunting methods of grey wolves (GWs). The hierarchy of GWs has four groups: alpha, beta, delta, and omegas. GWO selects the three fittest wolves (best solutions) as the alpha, beta, and delta, while the rest as omegas. The hunting process of GWs is guided by the three fittest wolves. All omegas follow them. It has four phases, which are mathematically modeled into four behaviors: Harassing Prey, Hunting, Attacking, and Searching, that create a high exploitative searching strategy. It quickly converges to an optimum solution for unimodal functions. However, it suffers from multimodal functions since it has a low explorative movement. Therefore, some variants of GWO are developed by incorporating various mechanisms/operators, such as differential evolution with elimination mechanism [24], simulated annealing [25], or refraction learning operator [26]. GWO can also be improved using a dimension learning-based hunting movement strategy [27], which uses a different approach to construct a neighborhood for each wolf to enhance the balance of local and global searches and maintain diversity.

In 2015, Ant Lion Optimizer (ALO) was proposed by Mirjalili [28]. ALO mimics the interaction between antlions and ants in the trap, where ants move over the search space and antlions hunt them and become fitter using traps. A new random walk is introduced to model the ant's movement as they move stochastically in nature to find some food. It has high exploitation and convergence speed because of the adaptive boundary shrinking mechanism and elitism. It also high exploration due to the random walk and roulette wheel selection mechanisms. However, although it has few parameters, some schemes and movements make ALO seems too-complicated. Hence, some versions of ALO are created by modifying, hybridizing, and providing an ability to solve a multi-objective problem [13].

In 2020, the metaphor-less optimization methods called Rao algorithms were proposed by Ravipudi Venkata Rao [29]. The Rao Algorithms use both best and worst solutions in each iteration and the random interactions among the candidate solutions to quickly find an optimum solution. They need two standard parameters: population size and a maximum number of evaluations that easy to adjust. They drop many parameters used in the previous metaphor-based algorithms, such as cohesion, intensity, probability, and other commonly challenging parameters to tune carefully.

The Rao algorithms have three variants: Rao-1, Rao-2, and Rao-3, which respectively use three different equations below:

$$X'_{j,k,i} = X_{j,k,i} + r_{1,j,i}(X_{j,\text{best},i} - X_{j,\text{worst},i}) \tag{1}$$

$$X'_{j,k,i} = X_{j,k,i} + r_{1,j,i}(X_{j,\text{best},i} - X_{j,\text{worst},i}) + r_{2,j,i}(|X_{j,k,i} \text{ or } X_{j,l,i}| - |X_{j,l,i} \text{ or } X_{j,k,i}|), \tag{2}$$

$$X'_{j,k,i} = X_{j,k,i} + r_{1,j,i}(X_{j,\text{best},i} - |X_{j,\text{worst},i}|) + r_{2,j,i}(|X_{j,k,i} \text{ or } X_{j,l,i}| - (X_{j,l,i} \text{ or } X_{j,k,i})), \tag{3}$$

where $X_{j,\text{best},i}$ represents the best candidate as the value of variable j, and $X_{j,\text{worst},i}$ represents the worst candidate as value of variable j, both throughout the ith iteration. $X'_{j,k,i}$ is the updated value after the equation, and both $r_{1,j,i}$ as well as $r_{2,j,i}$ are randomly generated in [0,1] for the jth variable throughout the ith iteration. In the term $|X_{j,k,i} \text{ or } X_{j,l,i}|$, the candidate solution k is compared to another candidate l, which is randomly selected from the available candidates in the population. The term $|X_{j,k,i}|$ is selected if k is fitter than l. Otherwise, the $|X_{j,l,i}|$ is chosen. The same rule is applied to the second term $(X_{j,l,i} \text{ or } X_{j,k,i})$.

All formulas used in the three Rao algorithms are similar to GWO, making them more exploitative than explorative. Using both best and worst solutions, they converge to an optimum solution for unimodal functions more quickly than GWO. However, with low explorative movement, they can be worse for multimodal functions. As described in [29], Rao is easy to get stuck in multimodal functions. Rao-3 gives a better solution in the Schwefel function from the six benchmark multimodal-functions and much worse for the other five benchmark multimodal-functions.

Therefore, in this research, an evolutionary Rao algorithm (ERA) is proposed to enhance the three original Rao algorithms by introducing two additional schemes. Firstly, the population is split into two subpopulations based on their qualities: high and low, with a particular portion depending on the given problem. The high-quality sub-population searches for an optimum solution in an exploitative manner using a movement scheme used in the Rao-3 algorithm. Meanwhile, the low-quality one does in an explorative fashion using a new random walk introduced in this research. This scheme is similar to the courtship learning framework in the Enhanced FA [21], where the population is also divided into two subpopulations: female and male, but ERA uses a predefined specific portion. Secondly, two evolutionary operators: crossover and mutation, are used to give exploitation and exploration searching strategies. A fitness-based adaptation is introduced to dynamically tune the portion of high-quality individuals, mutation radius, and mutation rate during the evolution. Meanwhile, the crossover is implemented using a random scheme with the common probabilistic values that do not create any additional parameters. The ERA is finally examined and compared to the three original Rao algorithms [29] as well as the firefly algorithm with courtship learning (FA-CL) [21] using three groups of benchmark functions: 1) the classic benchmark functions that contain seven unimodal, six multimodal, and ten low-dimension multimodal; 2) the CEC-C06 2019 test suites that consists of ten benchmark functions [30]; and 3) the global trajectory optimization problems provided by European Space Agency that contains five real problems of Cassini1, GTOC1, Messenger, Sagas, and Cassini2 [31].

2. Proposed evolutionary Rao algorithm

The pseudo-code of ERA is illustrated in Algorithm 1. In the initial phase, define the fixed population size p, the initial portion of high-quality (HQ) individuals $s = 0.5$, the initial mutation radius $a = 0.5$, the initial mutation rate $b = 0.9$, and randomly initialize the population of p individuals. In the next phase, the evolution is performed until a stopping condition is reached, such as when the number of evaluations is equal to the given maximum limit.

In each generation, six steps are carried out. Firstly, the quality of each individual is calculated; and their quality-ranks are then sorted in the descending mode. Secondly, the population is split into two sub-populations: high-quality (HQ) and low-quality (LQ), with the defined portion s, and both the best individual X_{best} and the worst individual X_{worst} are selected. Thirdly, each HQ individual is moved to follow the X_{best} using Eq. (3). Fourthly, the fittest HQ individual is selected as the BestHQ, and then one of the two evolutionary operators is chosen: crossover (exploitative) or mutation (explorative), to move the X_{best}. Fifthly, each LQ individual is moved using a new random walk. Finally, the fitness-based adaptation is performed by updating s, a, and b based on the improvement or stagnation of two consecutive best-so-far fitness.

Algorithm 1. Evolutionary Rao algorithm

Result: X_{best} as the optimum solution

Set p as the fixed population size (number of individuals);

Set $s = 0.5$, $a = 0.5$, and $b = 0.9$ as the initial values of high-quality (HQ) individuals portion, mutation radius, and mutation rate, respectively;

Randomly initialize the population of p individuals;

while *StoppingCondition* = *false* **do**

  for each individual, calculate its quality and then sort the quality-ranks in the descending mode;

  Select the fittest individual as the X_{best};

  Select the most fit individuals with the defined portion s as the HQ and the rests as the low-quality (LQ) individuals;

  Select the lowest-quality individual as the X_{worst};

  for each HQ individual, move it to follow the X_{best} using Eq. (3);

  Select the fittest HQ individual as the BestHQ;

  if *rand* > *0.5* **then**

    Offsprings = Crossover(BestHQ, X_{best});

    Replacement(BestHQ, X_{best}, Offsprings);

  else

    Offspring = Mutation(X_{best});

    Replacement(X_{best}, Offspring);

  end

  for each LQ individual move it to follow or distract a randomly selected HQ individual on the half of dimensions using Eq. (9);

  if *two consecutive best-so-far fitness show an improvement* **then**

    Increase s, but decrease a and b, using Eq. (10), (11), and (12);

  else

    Decrease s, but increase a and b, using Eq. (10), (11), and (12);

    Mutate $(1 - s) \times p$ low-quality individuals;

  end

end

2.1. Two sub-populations

The population of p candidate solutions (individuals) is split into two sub-populations based on their qualities: high and low, with a proper portion based on the given problem. The high-quality (HQ) sub-population searches for an optimum solution in an exploitative manner using the same movement scheme as in the Rao-3 algorithm. Meanwhile, the low-quality (LQ) one does in an explorative fashion using a new random walk introduced in this research. Hence, this scheme creates a new parameter s: the portion of high and low-quality individuals in the population. It is in the interval (0, 1) and easy to adjust. Hypothetically, it should be high (more than 0.5) to make ERA more exploitative and faster to optimize the unimodal functions. In contrast, it must be low (less than 0.5) to make ERA more explorative to solve the multimodal functions. A fitness-based adaptation scheme is proposed to increase or decrease the portion s automatically based on the best-so-far fitness during the evolution. If two consecutive best-so-far fitness values show an improvement, then the portion s is decreased to

make ERA more exploitative. In contrast, if two consecutive best-so-far fitness shows a stagnation, then the portion s is increased to make ERA more explorative. A detailed explanation will be provided in Section 2.5.

Furthermore, the population of p individuals is split into two sub-populations: the high-quality subpopulation of h individuals and the low-quality sub-population of l individuals, which are calculated as

$$h = \lfloor .(p-1) \times s \rfloor ., \tag{4}$$

$$l = (p-1) - h, \tag{5}$$

where s is the portion of HQ individuals in the population. However, both Eqs. (4) and (5) may produce zero for either h or l if the portion s is too-small or too-high. Hence, an enforcement procedure is implemented to ensure that a too-small s makes the HQ sub-population consists of at least two individuals, and a too-big s also makes the LQ sub-population contains at least two individuals.

2.2. Crossover

The crossover is implemented using a whole arithmetic crossover, which is defined as

$$\begin{aligned} X^{'} &= r \cdot X + (1-r) \cdot Y \\ Y^{'} &= r \cdot Y + (1-r) \cdot X \end{aligned} \tag{6}$$

where r is a randomly generated number in the interval (0, 1), which should be not equal to 0.5 to prevent generating the same two offsprings (new individuals); if $r = 0.5$, then both offsprings $X^{'}$ and $Y^{'}$ are the same as the average of both current individuals X and Y. Hence, this crossover scheme does not need any user parameter.

2.3. Mutation

The mutation is simply implemented using a creep mutation by adding a small value (positive or negative) to each mutated element. The small value is randomly generated using a Gaussian probability that is symmetric, distributed on 0, and has a high probability for the smaller values. The creep mutation is defined as

$$\langle x_1, x_2, \ldots, x_n \rangle \rightarrow \langle x_1^{'}, x_2^{'}, \ldots, x_n^{'} \rangle, \tag{7}$$

$$x_i^{'} = \begin{cases} x_i + (2r_1 - 1) \times a|U_i - L_i|, \text{ if } r_2 < b \\ x_i, \text{ otherwise}, \end{cases} \tag{8}$$

where $x_1, x_2, \ldots x_n \in [L_i, U_i]$, L_i and U_i are the lower and upper bounds of the interval of the ith element (variable or dimension), r_1 and r_2 are random values with the normal distribution in the interval [0, 1], and a and b are the mutation radius and the mutation rate, respectively, which are automatically tuned using a fitness-based adaptation scheme that will be described in Section 2.5.

2.4. Random walk

To provide an ability to search for an optimum solution in an explorative manner, each LQ individual is moved using a new random walk formulated as

$$X_{m,\mathrm{LQ},i}^{'} = X_{m,\mathrm{LQ},i} + r_{1,m,i}(X_{m,\mathrm{HQ},n} - X_{m,\mathrm{LQ},i}) \tag{9}$$

where $X_{m,\mathrm{LQ},i}$ and $X_{m,\mathrm{HQ},n}$ is the LQ individual i and the HQ individual n (randomly selected from the high-quality sub-population), respectively, and m is the randomly selected dimension; not all dimensions are used here to make this random walk more explorative.

2.5. Fitness-based adaptation scheme

Based on the above description, ERA has four parameters: population size p, portion s, mutation-radius a, and mutation-rate b. Hypothetically, p is the most robust parameter. In contrast, s, a, and b are estimated quite sensitive since they control the exploration strategy. Therefore, these three parameters are designed to be tuned adaptively during the evolution. A new simple fitness-based adaptation scheme based on the fitness values of the best-so-far individual is proposed for this purpose. If two consecutive best-so-far fitness values show an improvement, then s is increased, but both a and b are decreased, to make ERA more exploitative. In contrast, if two consecutive best-so-far fitness shows a stagnation, then s is decreased, both a and b are increased to make ERA more explorative, and all low-quality individuals are mutated using both new a and b to spread them in new locations. The increment and decrement are formulated as follow:

$$s^{'} = \begin{cases} s \times (1 - \dfrac{\Delta f_1 + \Delta f_2}{2}), \text{ if } \Delta f_1 > 0 \text{ and } \Delta f_2 > 0 \\ s \times 0.97, \text{ if } \Delta f_1 = 0 \text{ and } \Delta f_2 = 0 \end{cases} \tag{10}$$

$$a^{'} = \begin{cases} a \times 0.97, \text{ if } \Delta f_1 > 0 \text{ and } \Delta f_2 > 0 \\ a \times 1.03, \text{ if } \Delta f_1 = 0 \text{ and } \Delta f_2 = 0 \end{cases} \tag{11}$$

$$b^{'} = \begin{cases} b \times 0.97, \text{ if } \Delta f_1 > 0 \text{ and } \Delta f_2 > 0 \\ b \times 1.03, \text{ if } \Delta f_1 = 0 \text{ and } \Delta f_2 = 0 \end{cases} \tag{12}$$

where $\Delta f_1 = \frac{|f_1 - f_2|}{f_1}$ and $\Delta f_2 = \frac{|f_2 - f_3|}{f_2}$ are the first and the second differences

Table 1
Twenty three classic benchmark functions

Func	Name	Type	Dim	Range	f_{min}
CF1	Sphere	Unimodal	30	[− 100, 100]	0
CF2	Schwefel 2.22	Unimodal	30	[− 100, 100]	0
CF3	Schwefel 1.2	Unimodal	30	[− 100, 100]	0
CF4	Schwefel 2.21	Unimodal	30	[− 100, 100]	0
CF5	Rosenbrock	Unimodal	30	[− 30, 30]	0
CF6	Step	Unimodal	30	[− 100, 100]	0
CF7	Quartic	Unimodal	30	[− 1.28, 1.28]	0
CF8	Schwefel	Multimodal	30	[− 500, 500]	− 418.9829 × Dim
CF9	Rastrigin	Multimodal	30	[− 5.12, 5.12]	0
CF10	Ackley	Multimodal	30	[− 32, 32]	0
CF11	Griewank	Multimodal	30	[− 600, 600]	0
CF12	Penalized	Multimodal	30	[− 50, 50]	0
CF13	Penalized2	Multimodal	30	[− 50, 50]	0
CF14	Foxholes	LDM	2	[− 65, 65]	0.998
CF15	Kowalik	LDM	4	[− 5, 5]	0.0003
CF16	Six Hump Camel	LDM	2	[− 5, 5]	− 1.0316
CF17	Branin	LDM	2	[− 5, 5]	0.398
CF18	GoldStein-Price	LDM	2	[− 2, 2]	3
CF19	Hartman 3	LDM	3	[0, 1]	− 3.86
CF20	Hartman 6	LDM	6	[0, 1]	− 3.32
CF21	Shekel 5	LDM	4	[0, 10]	− 10.1532
CF22	Shekel 7	LDM	4	[0, 10]	− 10.4029
CF23	Shekel 10	LDM	4	[0, 10]	− 10.5364

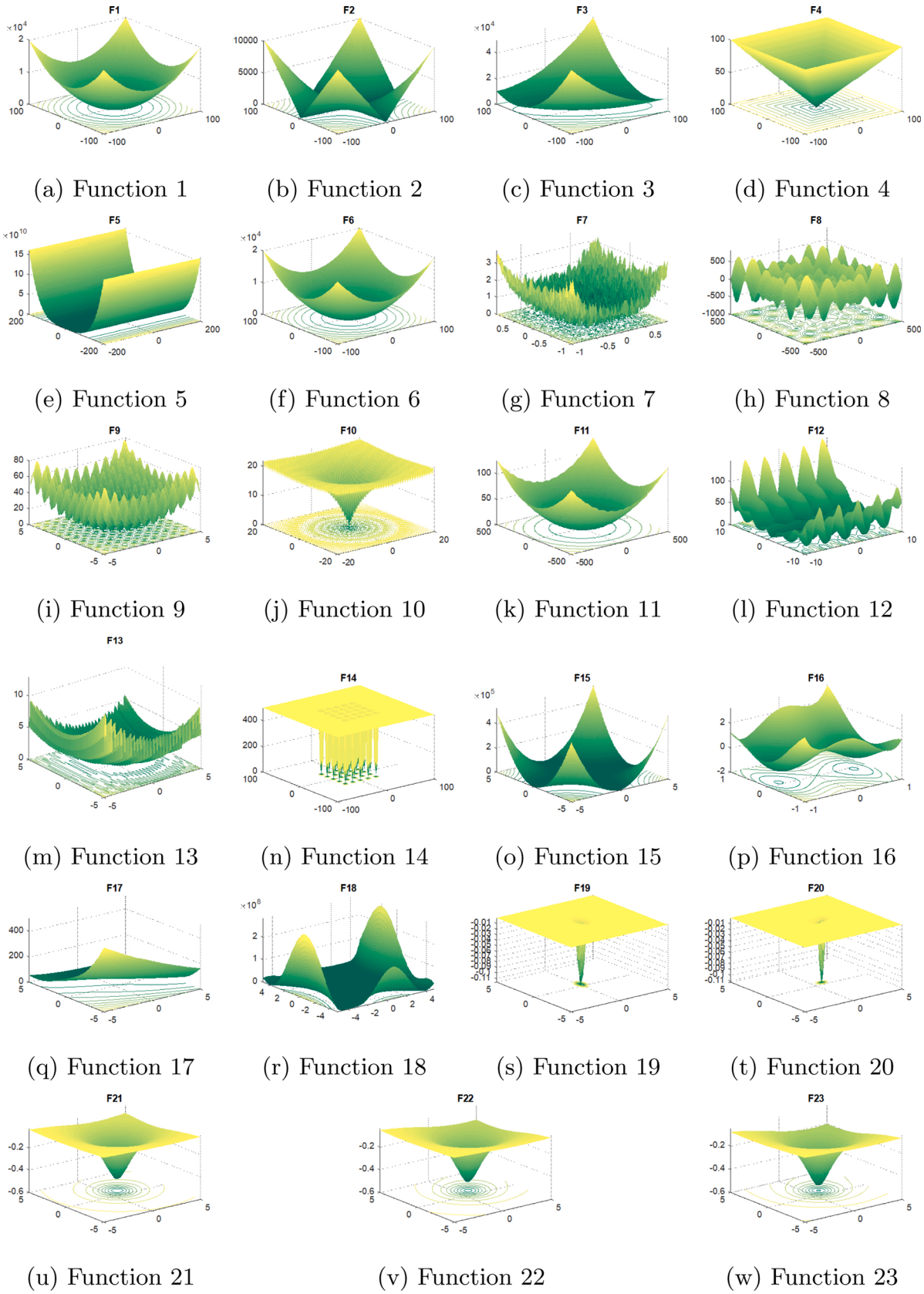

(a) Function 1 (b) Function 2 (c) Function 3 (d) Function 4

(e) Function 5 (f) Function 6 (g) Function 7 (h) Function 8

(i) Function 9 (j) Function 10 (k) Function 11 (l) Function 12

(m) Function 13 (n) Function 14 (o) Function 15 (p) Function 16

(q) Function 17 (r) Function 18 (s) Function 19 (t) Function 20

(u) Function 21 (v) Function 22 (w) Function 23

Fig. 1. Twenty three classic benchmark functions CF1 to CF23.

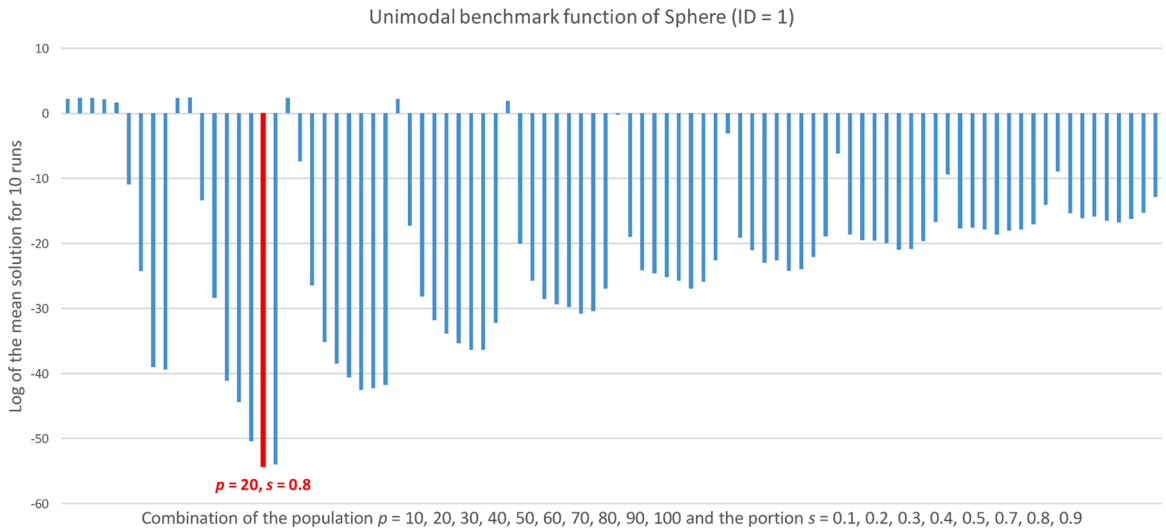

Fig. 2. Parameter tuning for a unimodal benchmark function of Sphere (ID = 1).

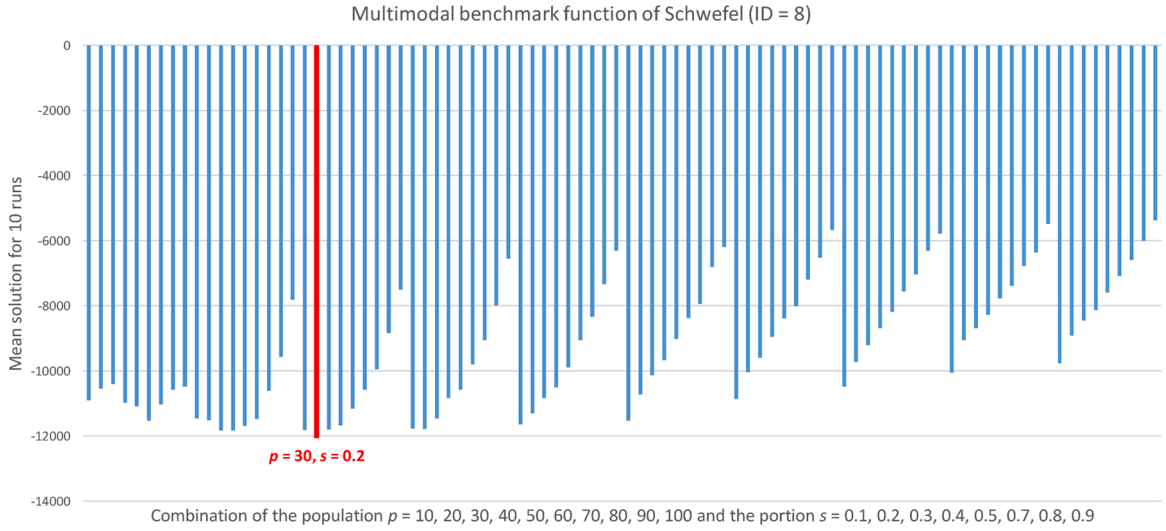

Fig. 3. Parameter tuning for a multimodal benchmark function of Schwefel (ID = 8).

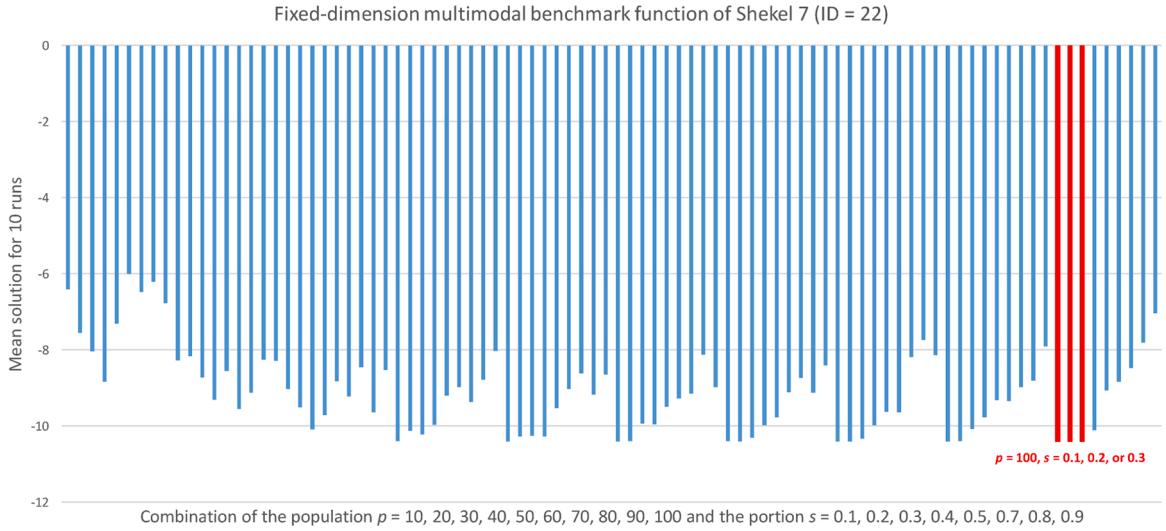

Fig. 4. Parameter tuning for a low-dimension multimodal benchmark function of Shekel 7 (ID = 22).

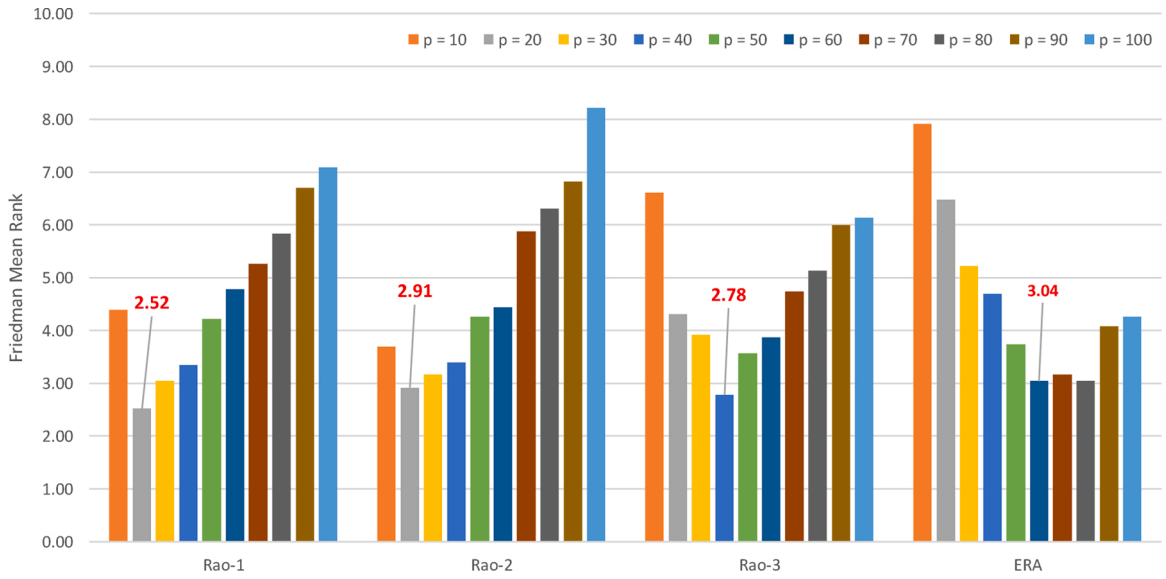

Fig. 5. Friedman mean rank calculated using 10 different population sizes p for each algorithm.

of the fitness values of two consecutive generations during the evolution process, respectively.

Moreover, the initial, minimum, and maximum values for those three parameters can be easily defined. Since the characteristics of the given problem are unknown, then the initial portion s is set as 0.5, while the minimum and the maximum values are set to 0.1 and 0.9, respectively. Next, both minimum and maximum values of a are set as 0.05 and 0.5, respectively. It means the mutation of an element (dimension) can occur in the radius of 5% to 50% out of the search space. In other words, an individual can be mutated at the maximum range of [-0.5, 0.5] in the search space. Hence, the mutation can cover the whole search space. Next, the initial value of a is tuned as 0.5 to provide the maximum exploration in the beginning iterations of the evolution process. Finally, b is defined in the interval [0.1, 0.9], and its initial value is 0.9 to maximize the exploration strategy in the beginning evolution process. Using the maximum mutation radius and rate, ERA can have a high-exploration ability to handle the effects of shift and rotation of the test functions, such as in the CEC-C06 2019 benchmark functions.

2.6. Complexity analysis of ERA

The mathematical complexity of ERA can be analyzed as follows. For each iteration, ERA has a time complexity of $O(p \times n + p \times c + logp)$, where p is the population size, n is the dimension of the given problem, c is the complexity of the objective function calculation, and $logp$ is the complexity of the fitness sorting to split the population into HQ and LQ sub-populations. It is clear that compared to the original Rao, ERA is slightly more complicated because of the additional sorting complexity of $logp$. Meanwhile, the complexity of the fitness-based adaptation scheme can be ignored since it is quite low; it only contains addition, substraction, and logical operations.

3. Results and discussion

In this research, twenty-three benchmark functions: seven unimodal, six multimodal, and ten low-dimension multimodal functions [29] are used to investigate both exploitation and exploration abilities of the proposed ERA. Table 1 illustrates the benchmark functions with their identities (ID), names, types, dimensions, ranges, and global optimum values $f_{\min}$. Meanwhile, their two-dimensional views are illustrated in Fig. 1. Seven benchmark functions, with ID = 1 to 7, are unimodal to examine the exploitation ability. Next, six benchmark functions, ID = 8 to 13, are multimodal, with many local optima increasing as the dimension increases, to evaluate the exploration ability. Finally, ten functions, ID = 14 to 23, are low-dimension multimodal (LDM) to investigate the exploration ability in the case of low-dimension optimization problems.

Table 2
Parameter settings.

Algorithm	Parameter settings
Rao-1	$p = 20$
Rao-2	$p = 20$
Rao-3	$p = 40$
FA-CL	$p = 20, \alpha = 0.5, \beta_{min} = 0.2, \beta = 1, \gamma = 1$
ERA	$p = 60, s = 0.5, a = 0.5, b = 0.9$

3.1. Preliminary observations

First, two parameters of ERA: population p and portion s, are observed to see their behaviors in optimizing the twenty-three classic benchmark functions. For each function, ninety experiments are performed using combination of 10 values of p = 10, 20, 30, 40, 50, 60, 70, 80, 90, 100 and nine values of s = 0.1, 0.2, 0.3, 0.4, 0.5, 0.7, 0.8, 0.9, which can be defined as pairs of (10, 0.1), (10, 0.2),..., (100, 0.9). For each experiment, the maximum number of function evaluations is set to 30,000 with ten runs to reduce the coincidence. Here, only three experimental results of the representative benchmark functions are shown and discussed, namely unimodal (Sphere, ID = 1), multimodal (Schwefel, ID = 8), and low-dimension multimodal (Shekel 7, ID = 22), to see the behaviors of both parameters p and s in optimizing those three types of benchmark functions. The common parameter value of p is finally selected as a fixed-optimum value for all the benchmark functions. Meanwhile, the portion s is dynamically updated during the evolution process using a fitness-based adaptation scheme.

Fig. 2 illustrates the experimental results for the problem of searching a minimum solution to a unimodal function of Sphere (ID = 1), where the vertical axis uses $\log(\text{meansolution})$ to ensure the bar chart clearly shows all results from the ninety experiments. It can be seen that a too-small (10) or a big population p (30–100) makes the ERA produces a bad solution. The bigger the p, the worse the solution. A small portion s (0.5 or less) also yields a poor solution. The smaller the s, the worse the

Table 3
Comparison of Rao-1, Rao-2, Rao-3, FA-CL, and ERA for 23 classic benchmark functions.

ID	Metric	Rao-1	Rao-2	Rao-3	FA-CL	ERA
1	Best	1.44026E-13	0.000206616	1.37198E-16	3360.332345	1.44407E-11
	Worst	1.56215E-11	0.05322429	3.57068E-13	7391.524099	7.07827E-10
	Mean	1.6427E-12	0.007910073	2.93612E-14	5494.642553	2.03341E-10
	STD	2.94821E-12	0.012500245	6.93888E-14	897.6329345	1.97333E-10
	MFE	30000	30000	30000	30176.8	30032
2	Best	9.88458E-08	0.046106637	3.48002E-09	20.78017429	2.1222E-06
	Worst	2.84524E-05	81.77760505	1.96246E-07	36.38814153	2.38276E-05
	Mean	1.75865E-06	6.122312306	4.70062E-08	31.53033206	8.63966E-06
	STD	5.11921E-06	16.17762336	5.36523E-08	3.444133931	4.73519E-06
	MFE	30000	30000	30000	30182.46667	30028.2
3	Best	29.58384537	24308.67108	5351.839864	6485.004266	983.5012373
	Worst	410.0667787	45693.37909	19092.21252	14405.71624	3470.902824
	Mean	149.4341504	35855.17634	11301.74245	10486.02575	2303.225697
	STD	105.4899095	5718.824871	3745.250011	1944.35227	728.8781476
	MFE	30000	30000	30000	30208.9	30023.6
4	Best	1.201443048	7.137837854	0.042098173	21.36789617	0.042019247
	Worst	12.36146637	28.08331631	59.65566877	36.06694776	0.300012918
	Mean	5.214910493	16.15411285	7.347592214	28.9938981	0.124708246
	STD	3.489736613	4.841469952	13.05854573	3.59291026	0.061288909
	MFE	30000	30000	30000	30226.43333	30025.6
5	Best	0.287292008	0.439075353	12.58554648	226704.144	18.30326575
	Worst	93.46438644	3019.406575	100.1684583	2564425.907	109.1279756
	Mean	35.67946414	130.9427468	35.87671438	1261919.835	31.40688996
	STD	29.6735389	546.4756884	27.26289807	584515.0346	17.69375467
	MFE	30000	30000	30000	30203.33333	30029.4
6	Best	2	0	0	3792	0
	Worst	53	12	3	7639	2
	Mean	10.2	1.833333333	0.3	5555.266667	0.2
	STD	9.219170432	3.006697505	0.651258728	1099.28108	0.484234198
	MFE	30000	28073.33333	13776	30144.96667	12368
7	Best	0.03452811	0.03404685	0.005036199	1.530176956	0.004682426
	Worst	0.211389877	0.168091645	0.081089247	4.106762973	0.036293801
	Mean	0.080890625	0.093085738	0.019933199	2.624059197	0.013211183
	STD	0.036979081	0.031284187	0.016182882	0.659081008	0.007750259
	MFE	30000	30000	30000	30145.5	30027.2
8	Best	− 10682.09946	− 10239.35633	− 11345.58004	− 4377.087113	− 8879.935043
	Worst	− 3893.432932	− 5125.91502	− 3869.781006	− 3291.297315	− 6882.950077
	Mean	− 6470.266849	− 8027.033295	− 8325.725086	− 3701.706264	− 7753.907755
	STD	2090.801691	1321.261016	2361.956999	288.5432924	413.9236488
	MFE	30000	30000	30000	30163.16667	30038.8
9	Best	82.58144051	183.9047143	174.6873065	189.5462566	11.82239455
	Worst	275.100287	283.1739045	249.2618453	242.3410246	44.09695302
	Mean	211.4806106	238.8109701	203.3125985	216.0038257	29.26076862
	STD	41.58262643	25.05505101	17.48088927	12.57640716	7.210275076
	MFE	30000	30000	30000	30246.93333	30033.6
10	Best	1.340421288	0.01602575	4.51465E-09	11.80926578	9.14087E-07
	Worst	19.96317829	19.96048248	0.931304602	13.48685262	1.87018E-05
	Mean	3.544848527	6.029369132	0.062087072	12.71855001	4.61579E-06
	STD	4.523133052	8.827128996	0.236279524	0.503095444	3.42908E-06
	MFE	30000	30000	30000	30174.03333	30034.8
11	Best	3.87024E-13	0.000684082	4.67404E-14	18.67629168	5.55651E-11
	Worst	0.070984139	0.741672368	0.569327929	68.09827573	0.343918782
	Mean	0.016380538	0.480608522	0.125402819	41.81819117	0.093842602
	STD	0.016674644	0.220909193	0.12739394	11.89438954	0.089296594
	MFE	30000	30000	30000	30176.23333	30034.8
12	Best	2.95944E-12	0.101041766	0.320579961	1112.053147	0.031510408
	Worst	25.77634972	15.3687038	2.587976377	219089.505	2.00220998
	Mean	3.326291084	5.096597329	0.818413527	48693.6658	0.37438139
	STD	5.791910477	3.953017932	0.57337885	53495.37265	0.390735094
	MFE	30000	30000	30000	30234.96667	30038.6
13	Best	1.46599E-12	4.87385E-12	2.56084E-17	75765.28964	1.87724E-08
	Worst	40.25456675	48.02336319	0.09737116	4583252.205	0.240192154
	Mean	8.886192319	4.13473568	0.011985054	1560315.509	0.02981008
	STD	12.0496735	11.2745274	0.025838424	994963.699	0.062183659
	MFE	30000	30000	30000	30238.76667	30035
14	Best	0.998003838	0.998003838	0.998003839	0.998055928	0.998003838
	Worst	0.998003838	0.998004194	0.999925881	3.968250346	0.998003843
	Mean	0.998003838	0.998003852	0.998257477	1.808262855	0.998003838
	STD	1.23698E-16	6.49804E-08	0.000527552	0.810513825	9.98569E-10
	MFE	30000	30000	30000	30199.9	30035.2
15	Best	0.000307486	0.000307486	0.000324243	0.001364568	0.000424113
	Worst	0.020434946	0.008333703	0.001272374	0.009562903	0.001380486
	Mean	0.00454563	0.001289295	0.000596688	0.004038841	0.000701339
	STD	0.008058756	0.001977607	0.000244477	0.002218998	0.000213724

(*continued on next page*)

Table 3 (*continued*)

ID	Metric	Rao-1	Rao-2	Rao-3	FA-CL	ERA
	MFE	30000	30000	30000	30297.76667	30030
16	Best	− 1.031628054	− 1.031628233	− 1.03162617	− 1.031552471	− 1.031627676
	Worst	− 1.031584914	− 1.03155237	− 1.031600346	− 1.011904581	− 1.031602254
	Mean	− 1.031611222	− 1.031611907	− 1.031611279	− 1.028544595	− 1.031615743
	STD	1.08599E-05	1.47749E-05	7.75488E-06	0.003767043	8.22898E-06
	MFE	7041.333333	7202	8500	30176.5	2338
17	Best	0.397894345	0.397887438	0.397897956	0.397910357	0.397888025
	Worst	0.397999462	0.397996151	0.397988112	0.457108975	0.397998161
	Mean	0.397945174	0.397940169	0.39794788	0.407336514	0.397952448
	STD	2.93566E-05	3.44684E-05	2.58238E-05	0.012636874	3.35746E-05
	MFE	595.3333333	465.3333333	896	29274.23333	1524
18	Best	3	3	3.00001234	3.00144078	3
	Worst	3	3	3.002994418	3.461306359	3
	Mean	3	3	3.00043706	3.132162867	3
	STD	1.90941E-14	1.4162E-14	0.000581165	0.111886989	2.35699E-13
	MFE	2750.666667	6644	30000	30283.56667	13147.6
19	Best	− 3.862647264	− 3.862646836	− 3.862630337	− 3.86273971	− 3.862476872
	Worst	− 3.860015745	− 3.860014013	− 3.860166138	− 3.814862203	− 3.860018537
	Mean	− 3.861284579	− 3.860875224	− 3.861230723	− 3.847444698	− 3.861305717
	STD	0.000759734	0.000609944	0.000769165	0.01227268	0.000744026
	MFE	526	326.6666667	721.3333333	29257.36667	1496
20	Best	− 3.321514906	− 3.321517556	− 3.321340804	− 3.232776201	− 3.3216568
	Worst	− 3.190272286	− 3.20310205	− 3.20310205	− 2.774548607	− 3.18590451
	Mean	− 3.271481418	− 3.27357853	− 3.257887186	− 2.964897304	− 3.283422687
	STD	0.058118203	0.058528253	0.059569551	0.119154691	0.056560408
	MFE	15438	12787.33333	16832	30262.93333	14456.4
21	Best	− 10.15319968	− 10.15319968	− 10.15319968	− 9.237961427	− 10.15319968
	Worst	− 4.051730311	− 2.630471668	− 2.630471668	− 2.348276139	− 3.873011974
	Mean	− 7.571532266	− 7.286516369	− 7.988655139	− 5.13102673	− 8.758677601
	STD	2.183528248	2.791706593	2.300114085	2.319287801	2.257015113
	MFE	30000	30000	30000	30201.03333	30029.6
22	Best	− 10.40293072	− 10.40293811	− 10.40293612	− 10.26936583	− 10.40292495
	Worst	− 3.724300347	− 1.837592971	− 7.655316059	− 2.356385661	− 4.785539658
	Mean	− 8.513729479	− 9.193001948	− 10.14971362	− 5.773917362	− 9.962990885
	STD	2.516505404	2.672409474	0.667381659	2.772503044	1.251621589
	MFE	19810	7462.666667	10530.66667	30195.36667	28090
23	Best	− 10.53640962	− 10.53640895	− 10.53640895	− 9.998537379	− 10.53640573
	Worst	− 5.032711076	− 2.421734027	− 2.4273352	− 2.420451607	− 3.835426802
	Mean	− 9.76293601	− 8.189952935	− 9.457598582	− 5.207676489	− 10.10837656
	STD	1.635492849	3.653678401	2.385255584	2.37062617	1.331195279
	MFE	18558.66667	10478	11730.66667	30157.76667	27428.6
	FMR	2.43	3.17	2.13	4.83	1.52
	Rank	3	4	2	5	1

solution. Hence, the combination of a too-big p and a too-small s is not recommended. The optimum combination is reached on $p = 20$ and $s = 0.8$. This result proves that a big portion of high-quality individuals in the small population makes the proposed ERA more exploitative and faster to find the optimum solution.

Next, Fig. 3 illustrates the ninety experimental results for the problem of minimizing a multimodal function of Schwefel (ID = 8). It informs that the portion s is sensitive, but the population size p is not; the bigger the s, the worse the solution. A too-big portion s drastically reduces the solution quality. The optimum combination is reached on $p = 30$ and $s = 0.2$. This result proves that a small portion of high-quality individuals in the small population makes the proposed ERA more explorative and faster to find the optimum solution to the multimodal functions with many local optima.

Finally, Fig. 4 illustrates the ninety experimental results for the problem of minimizing a low-dimension multimodal function of Shekel 7 (ID = 22). It also informs that the portion s is sensitive, but the population size p is not; the bigger the s, the worse the solution. A too-big portion s drastically reduces the solution quality. The optimum combination is reached on a big $p = 100$ and a low $s = 0.2$. However, a smaller p up to 20 or 30 also gives a good solution. This result informs that a small portion of high-quality individuals in the big population makes ERA more explorative. Hence, it can search for an optimum solution to the low-dimension multimodal functions with a wide flat area.

The three observations above prove the hypothesis that p is more robust than s. Therefore, the adaptation scheme is applied on s instead of p. A fitness-based adaptation of population size introduced in [32] is reported can improve the performance of the differential evolution, but that scheme is not used here since it will increase the complexity of ERA. Thus, p is designed to be a fixed value and tuned manually by doing a few experiments.

3.2. Parameter settings

Based on the research in [21], the best population size for FA-CL is 20. Thus, the parameter setting is focused on Rao-1, Rao-2, Rao-3, and ERA. Here, ten experiments with $p = 10, 20, \ldots, 100$ are carried out to find the optimum p for each algorithm based on the Friedman Mean Rank (FMR).

Fig. 5 illustrates the experimental results. The behavior of p is similar for Rao-1 and Rao-2. The smaller the p, the better the rank. The optimum value is reached on $p = 20$ for both algorithms. Meanwhile, p gives a different effect for Rao-3 that achieves the optimum value on $p = 40$. It also shows the different impacts for ERA, which gets the optimum value on $p = 60$. Finally, the parameter settings for ERA and other algorithms are listed in Table 2.

Table 4
The *p*-values of Wilcoxon rank sum test (WRST) for 23 classic benchmark functions.

ID	ERA vs Rao-1	ERA vs Rao-2	ERA vs Rao-3	ERA vs FA-CL
1	3.68973E-11	3.01986E-11	3.01986E-11	3.01986E-11
2	8.89099E-10	3.01986E-11	3.01986E-11	3.01986E-11
3	3.01986E-11	3.01986E-11	3.01986E-11	3.01986E-11
4	3.01986E-11	3.01986E-11	4.57257E-09	3.01986E-11
5	0.027086318	0.115362360	0.000526404	3.01986E-11
6	5.29270E-12	0.002309997	0.537496020	5.18120E-12
7	3.33839E-11	3.33839E-11	0.022360148	3.01986E-11
8	0.000421751	0.105469947	0.065671258	3.01986E-11
9	3.01986E-11	3.01986E-11	3.01986E-11	3.01986E-11
10	3.01986E-11	3.01986E-11	8.48477E-09	3.01986E-11
11	8.66343E-05	2.01522E-08	0.501143668	3.01986E-11
12	0.040595001	1.28704E-09	3.83067E-05	3.01986E-11
13	0.009883401	0.013271805	0.001766564	3.01986E-11
14	0.405861585	9.89193E-09	6.4749E-120	5.21903E-12
15	0.318136088	0.529748183	0.074827008	3.33839E-11
16	0.093340797	0.420386330	0.055545693	3.01986E-11
17	0.437641335	0.157975689	0.510597937	4.19968E-10
18	0.036392066	0.812931300	3.01041E-11	3.01041E-11
19	0.935191970	0.022360148	0.641423523	1.42942E-08
20	0.369977675	0.110560585	0.659705270	7.38908E-11
21	0.283376373	0.425345373	0.578792661	4.44405E-07
22	0.923442132	0.000556012	5.97056E-05	1.28704E-09
23	0.003670893	0.019094054	0.001235991	4.19968E-10

3.3. Evaluation on classic benchmark functions

First, the proposed ERA is examined and compared with four other algorithms: Rao-1, Rao-2, Rao-3, and FA-CL to search the minimum solutions to the twenty-three benchmark functions listed in Table 1. For each benchmark function, the maximum number of function evaluations is set to 30,000 with 30 runs to reduce the coincidence. The random seeds of the 30 initial populations (for each benchmark function) are the same when the algorithms use the same population size p to get fairness. Otherwise, they are different. The Matlab source-codes used in the Rao-1, Rao-2 and Rao-3 refer to [29] while the one used in FA-CL refers to [21]. Meanwhile, the optimum parameter settings for all algorithms are described in Section 3.2. Table 3 illustrates the examination results based on five metrics (Met): best solution, worst solution, mean solution, standard deviation (STD), and mean function evaluations (MFE).

Based on the two metrics, mean solution and STD, for the seven unimodal functions, ID = 1 to 7, the proposed ERA commonly outperforms all the other algorithms for the four functions with ID = 4, 5, 6, and 7. Unfortunately, it is worse than Rao-3 and Rao-1 for two functions with ID = 1 and 2. Besides, it is much worse than Rao-1 for the function ID = 3.

Next, the investigation on the six multimodal functions, ID = 8 to 13, informs that the proposed ERA also generally outperforms the competitors, where it achieves much lower mean solutions for three functions with ID = 9, 10, and 12. It is slightly worse than Rao-3 and Rao-2 for the

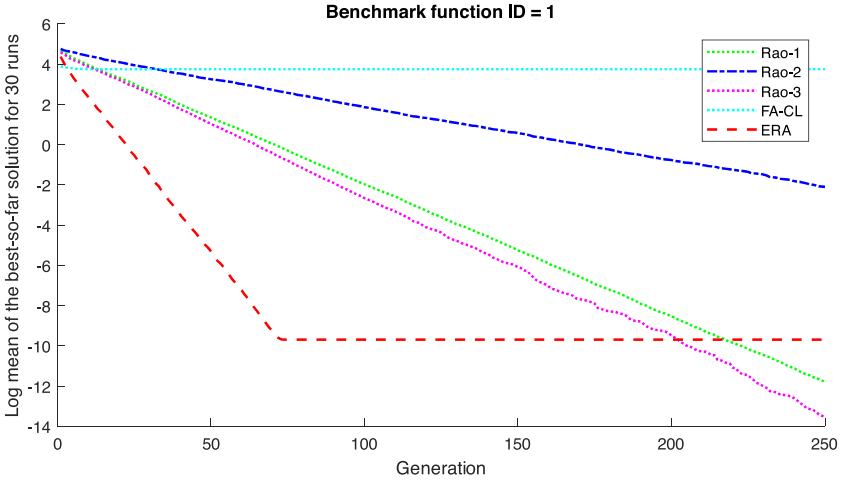

Fig. 6. Convergence analysis for a unimodal benchmark function of Sphere (ID = 1).

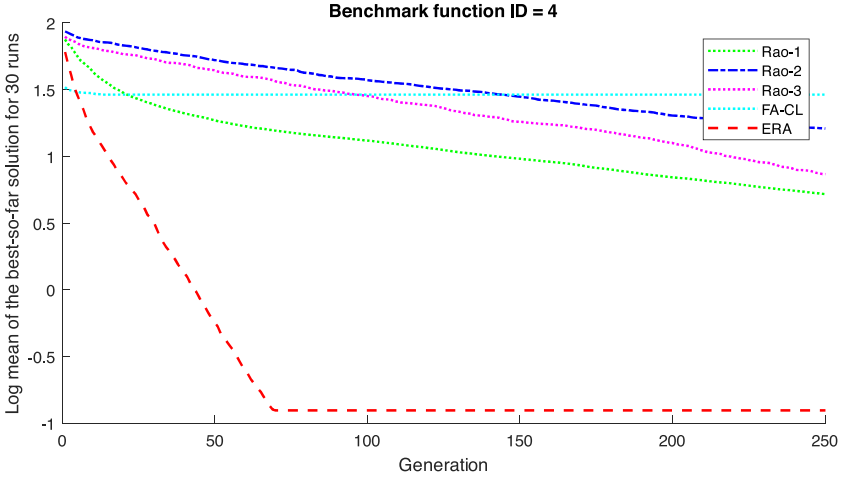

Fig. 7. Convergence analysis for a unimodal benchmark function of Schwefel 2.21 (ID = 4).

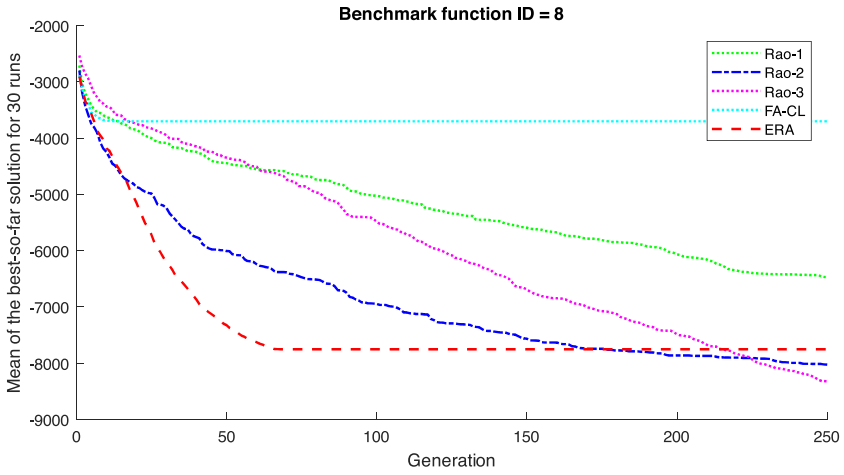

Fig. 8. Convergence analysis for a multimodal benchmark function of Schwefel (ID = 8).

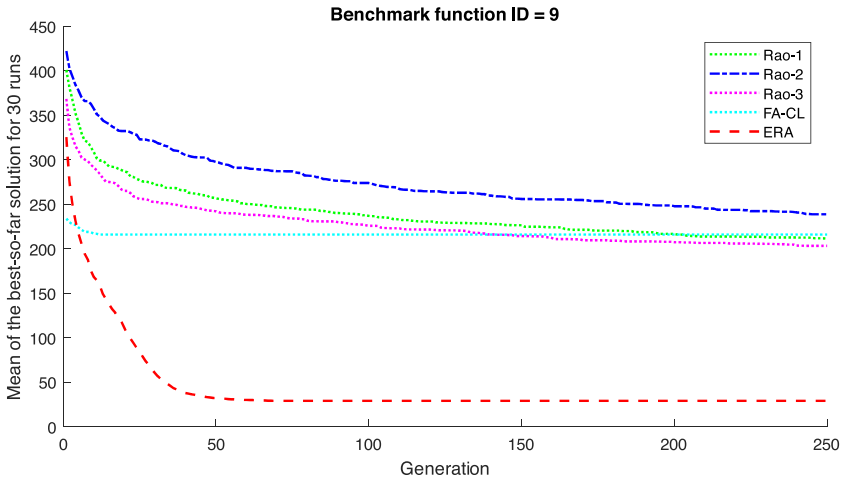

Fig. 9. Convergence analysis for a multimodal benchmark function of Rastrigin (ID = 9).

function ID = 8. It is much worse than Rao-1 and Rao-3 for the function ID = 11 and 13, respectively.

Finally, the investigation on the ten low-dimension multimodal functions, ID = 14 to 23, shows that the proposed ERA mostly gives better or equal mean solutions than the competitors. It reaches the best solutions for the three benchmark functions with ID = 20, 21 and 23. It gives the same or similar global solutions, with quite low MFE, as the three Rao algorithms for the benchmark function with ID = 16, 17, 18, and 19. It is slightly worse than Rao-1 or Rao-3 only for three benchmark functions (ID = 14, 15, and 22).

As a summary, based on Table 3, ERA reaches better mean solutions than all the competitors for 10 benchmark functions. It gives the same

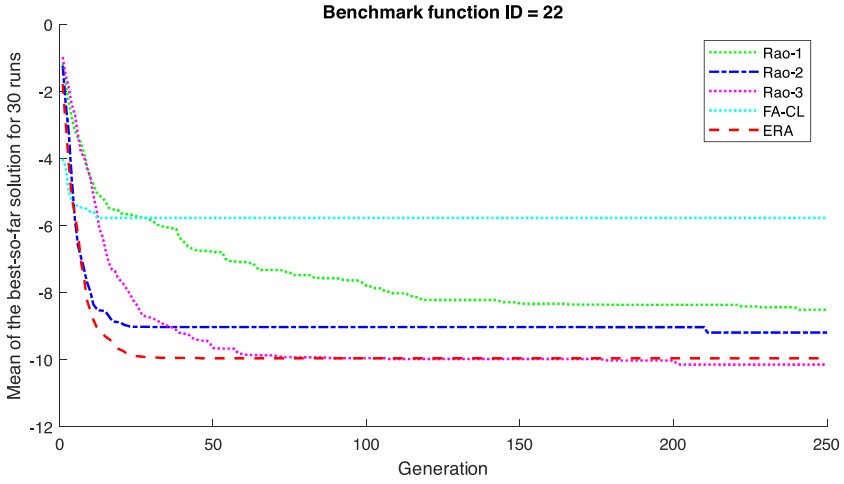

Fig. 10. Convergence analysis for a multimodal benchmark function of Shekel 7 (ID = 22).

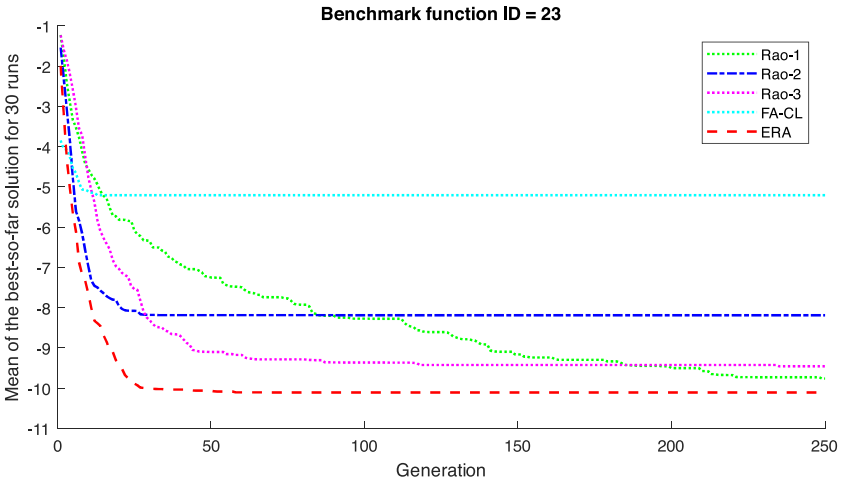

Fig. 11. Convergence analysis for a multimodal benchmark function of Shekel 10 (ID = 23).

and worse mean solutions for 4 and 9 benchmark functions, respectively. Statistically, based on the Friedman mean rank (FMR), ERA gives the highest performance with the lowest FMR of 1.52. The Wilcoxon rank-sum test (WRST) illustrated in Table 4 confirms that ERA is significantly better than all the competitors for the six benchmark functions (ID = 4, 7, 9, 10, 12, and 23), where all the *p*-values are less than 0.05. Meanwhile, for the four benchmark functions (ID = 5, 6, 20, and 21), ERA is only significantly better than some competitors but not for the others.

Moreover, the detailed investigations are then provided by the convergence curve analysis. The three subsections below discuss the convergence curves in detail for three benchmark groups: high-dimensional unimodal, high-dimensional multimodal, and low-dimensional multimodal.

3.3.1. *Investigation on 30-dimensions unimodal functions*

A detailed investigation of the seven 30-dimensions unimodal benchmark functions, ID = 1 to 7, is discussed by illustrating two convergence analyses of the proposed ERA and all the competitors. For each benchmark function, the maximum number of function evaluations is set to 30,000 with 30 runs to reduce the coincidence.

Fig. 6 shows the evolution of all the algorithms until convergence to the optimum solution for the benchmark function of Sphere (ID = 1). The horizontal axis is the generation, calculated as 30,000 function evaluations divided by the population size p. The random seeds of the 30 initial populations are the same for the algorithms that use the same optimum population size p. Hence, in this case, Rao-1, Rao-2, and FA-CL use the same initial population since they have the same optimum p = 20. In contrast, the Rao-3 and ERA use a different initial population because they have the optimum p = 40 and p = 60, respectively. Due to the different optimum p for each algorithm, the evolution is illustrated using the different step sizes of generation to get fairness. Here, the proposed ERA uses a step size of 2, Rao-3 uses 3, and the rests use 6 so that all the algorithms show the same generations of 1 to 250. It can be seen in Fig. 6 that the ERA is worse than Rao-1 and Rao-3. This result also applies to two other similar unimodal functions ID = 2 and 3.

Fig. 7 shows the evolution of all the algorithms for the benchmark function of Schwefel 2.21 (ID = 4). ERA converges much faster than the others. It converges in the one-fourth of the evolution, and, at the end of evolution, it gives the lowest mean solution compared to Rao-1, Rao-2, Rao-3, and FA-CL that produce much worse solutions. Similar results also happen to three other unimodal functions ID = 5, 6, and 7.

3.3.2. *Investigation on 30-dimensions multimodal functions*

Next, a detailed investigation of the six 30-dimensional multimodal benchmark functions, ID = 8 to 13, is illustrated by two convergence analyses of the proposed ERA and all other algorithms. Fig. 8 shows the convergence curves for the multimodal function of Schwefel (ID = 8) that has many local minima. ERA performs a little worse than Rao-1 and Rao-3, where it converges to a slightly bigger solution. This result also applies to two other multimodal functions (ID = 11 and 13).

Next, the convergence analysis is provided for the multimodal function of Rastrigin with ID = 9 that also has many local minima. Fig. 9 illustrates that the ERA converges much faster than the others. It evolves quickly in the beginning generations and gives the lowest mean solution among the competitors at the end of evolution. ERA also converges similarly for two other unimodal functions with ID = 10 and 12.

3.3.3. *Investigation on low-dimension multimodal functions*

Finally, the detailed investigations of ten benchmark low-dimension multimodal functions, ID = 14 to 23, are also illustrated by some convergence analyses of ERA and the competitors. Fig. 10 shows the evolution of all the algorithms for the 4-dimensions multimodal function of Shekel 7 (ID = 22) that has broad flat areas. In this case, ERA converges to a similar solution to Rao-3.

Furthermore, the convergence analysis is carried out for the 4-dimensions multimodal function of Shekel 10 (with ID = 23) with broad flat areas. Fig. 11 shows that ERA performs the best evolution and converges to a better solution than the competitors. This result also applies to three other low-dimensions multimodal functions with ID = 14, 15, and 21. Meanwhile, ERA gives the same (or similar) convergence curves as the competitors for 16, 17, 18, 19, and 20.

Those results of FMR, WRST, and convergence curves indicate that ERA generally outperforms all the competitors. It proves that the proposed schemes: two sub-populations and evolutionary operators equipped with the adaptation procedure can effectively control the exploration and exploitation balance. The detailed investigations on the fitness-based adaptation scheme will be given in Section 3.6.

3.4. *Evaluation on CEC-C06 2019*

The CEC-C06 2019 is a set of ten modern benchmark functions, namely CEC01, CEC02,..., CEC10. As described in [30], all the functions are scalable. The seven functions (CEC04 to CEC10) are shifted and rotated, but the others (CEC01 to CEC03) are not. Those seven functions are set as 10-dimensional minimization problems in the interval [− 100, 100] while the rests have different dimensions of 9, 16, and 18 in the interval [− 8192, 8192], [− 16384, 16384], and [− 4, 4], respectively. Besides, all ten benchmarks have the same global optimum of 1.

The proposed ERA is evaluated using those ten CEC-C06 2019 benchmarks, where their Matlab codes refer to [30], to see its ability to handle the effects of shift and rotation of the test functions. It is also

Table 5
Comparison of Rao-1, Rao-2, Rao-3, FA-CL, and ERA for ten benchmarks of CEC-C06 2019.

ID	Metric	Rao-1	Rao-2	Rao-3	FA-CL	ERA
CEC01	Best	390354788.1	2916410938	1456657938	20718576008	25205057.57
	Worst	18579735758	26602967009	22606057356	3.52496E+11	4087331440
	Mean	2969561815	12158813001	8150847618	1.24685E+11	873534390.1
	STD	3458651870	6343181227	6050933807	88017205415	854049190.6
	MFE	30000	30000	30000	30258.9	30034.8
CEC02	Best	17.34285714	17.34285714	17.39624973	985.6431507	17.34385166
	Worst	17.34285714	17.34285714	17.46552571	3599.0291	17.38067398
	Mean	17.34285714	17.34285714	17.43100117	2309.760136	17.35587136
	STD	7.04391E-15	6.66287E-15	0.019863442	686.3489262	0.008533771
	MFE	30000	30000	30000	30167.6	30050
CEC03	Best	12.70240422	12.70240422	12.70240422	12.70243367	12.70240422
	Worst	12.70251646	12.70252446	12.70253809	12.70313897	12.70240457
	Mean	12.70241519	12.70242315	12.70243599	12.70275408	12.70240423
	STD	2.61665E-05	3.04861E-05	3.51307E-05	0.000177661	6.36292E-08
	MFE	30000	30000	30000	30194.93333	30036.4
CEC04	Best	28.09976484	30.65215071	161.5987987	1416.884608	12.6848588
	Worst	55.30958498	67.28669199	293.2794152	7138.324036	137.9261529
	Mean	39.24039894	48.18340414	214.1502774	3937.361268	42.30643978
	STD	6.336978985	8.897804689	35.66651224	1184.043609	30.04084127
	MFE	30000	30000	30000	30215.03333	30032.4
CEC05	Best	1.280029538	1.40996188	1.5745926	1.943716683	1.025782758
	Worst	1.698018753	2.006177027	1.97844018	2.898249478	1.401388266
	Mean	1.521217618	1.676196554	1.810647002	2.607524	1.152216958
	STD	0.129249904	0.115365294	0.087314766	0.244163606	0.089725781
	MFE	30000	30000	30000	30205.93333	30042
CEC06	Best	9.733872974	9.387891192	8.762132719	10.44553117	9.112980123
	Worst	11.45221129	11.28957571	11.75705625	13.24136925	10.88436736
	Mean	10.56696371	10.46733143	10.51740995	12.09261107	10.03315348
	STD	0.440170202	0.509698432	0.686756457	0.804138499	0.496448922
	MFE	30000	30000	30000	30177.5	30040.4
CEC07	Best	272.7315304	155.7756802	286.8881473	349.6263842	155.6301339
	Worst	909.7970404	873.1138007	971.9938573	1424.750579	623.6837399
	Mean	621.4329426	523.9535639	619.1594318	982.5206281	397.7660801
	STD	182.4620119	177.2735789	175.8854884	241.0657041	115.7688378
	MFE	30000	30000	30000	30189.7	30055.6
CEC08	Best	5.3786702	5.158716685	4.494612984	5.437849384	2.610104398
	Worst	6.875548609	6.47014268	6.121359357	7.20917994	5.372692569
	Mean	6.000536425	5.812160004	5.518584178	6.554942645	4.300037284
	STD	0.355903577	0.33238346	0.394227163	0.415653324	0.742690621
	MFE	30000	30000	30000	30155.36667	30048.2
CEC09	Best	2.344511638	2.410388957	8.415440069	107.8777016	2.471916423
	Worst	2.364279095	2.678458436	106.5608922	876.6191415	18.25738167
	Mean	2.352775129	2.519079794	47.78092232	560.843819	4.325248722
	STD	0.004691204	0.063901687	21.70671343	192.3434718	2.804045367
	MFE	30000	30000	30000	30187.13333	30044.2
CEC10	Best	20.14320415	20.24340503	20.12140073	20.09700221	20.14872943
	Worst	20.57898412	20.52293164	20.59178469	20.77386591	20.49628839
	Mean	20.42696562	20.40786804	20.42908964	20.60276541	20.34605205
	STD	0.082810151	0.073689655	0.085669202	0.131641593	0.072081928
	MFE	30000	30000	30000	30155.63333	30027.6
	FMR	2.40	2.50	3.50	5.00	1.50
	Rank	2	3	4	5	1

Table 6
The *p*-values of Wilcoxon rank sum test (WRST) for ten benchmark functions of CEC-C06 2019.

ID	ERA vs Rao-1	ERA vs Rao-2	ERA vs Rao-3	ERA vs FA-CL
CEC01	1.33668E-05	3.68973E-11	6.72195E-10	3.01986E-11
CEC02	2.36384E-12	6.31878E-12	3.01986E-11	3.01986E-11
CEC03	0.065461305	1.01761E-05	1.77301E-09	3.01986E-11
CEC04	0.053685253	0.004856016	3.01986E-11	3.01986E-11
CEC05	8.99341E-11	3.01986E-11	3.01986E-11	3.01986E-11
CEC06	0.000212646	0.002156638	0.001370333	9.91863E-11
CEC07	1.09069E-05	0.005322078	4.7445E-06	2.37147E-10
CEC08	3.01986E-11	7.38908E-11	4.99795E-09	3.01986E-11
CEC09	3.01986E-11	4.19968E-10	3.68973E-11	3.01986E-11
CEC10	5.60728E-05	0.00185748	3.59234E-05	7.38029E-10

compared with the four other algorithms in their best performances using the parameter settings described in Section 3.2. All algorithms are run 30 times with 30,000 function evaluations each to get meaningful statistical results. Moreover, both FMR and WRST with the *p*-values are also provided. The experimental results illustrated in Table 5 show that ERA outperforms all the competitors for most benchmark functions. It reaches significantly better mean solutions for 7 out of 10 benchmarks: CEC01, CEC03, CEC05, CEC06, CEC07, CEC08, and CEC10. It gives little worse solutions than Rao-1 and Rao-2 for only three benchmarks: CEC02, CEC04, and CEC09. The Friedman mean rank shows that ERA is the first rank, where it achieves the lowest FMR of 1.50. Meanwhile Rao-1, Rao-2, Rao-3, and FA-CL give much worse FMR of 2.40, 2.50, 3.50, and 5.00, respectively.

Moreover, the Wilcoxon rank-sum test illustrated in Table 6 confirms that ERA is significantly better than all the competitors for the seven benchmark functions, where all the *p*-values are lower than the significance level of 0.05, except for the CEC03 where ERA is not significantly better than Rao-1. In contrast, for CEC02, ERA is slightly worse than

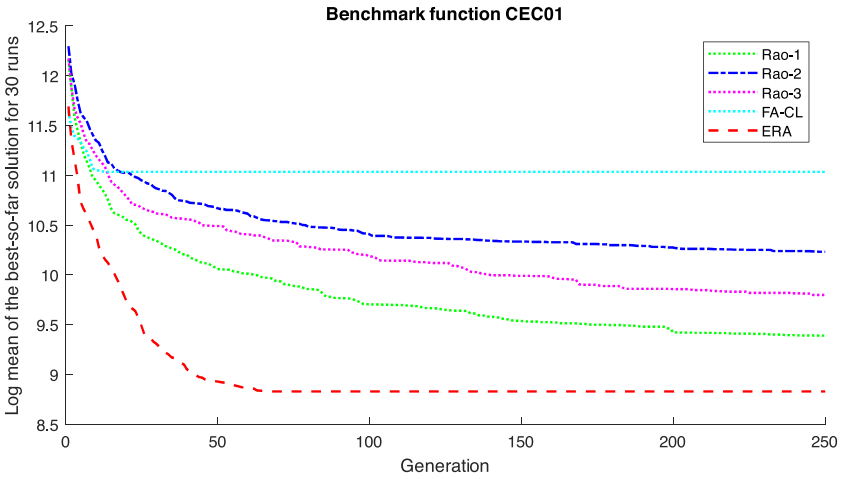

Fig. 12. Convergence analysis for CEC01.

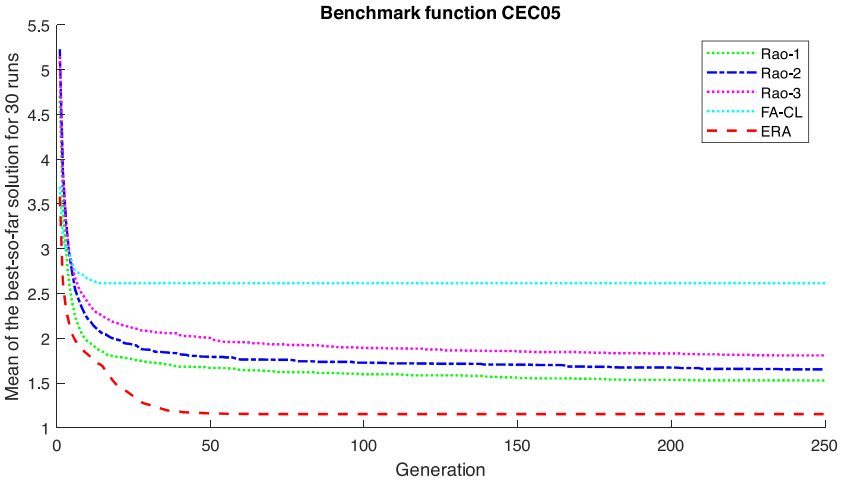

Fig. 13. Convergence analysis for CEC05.

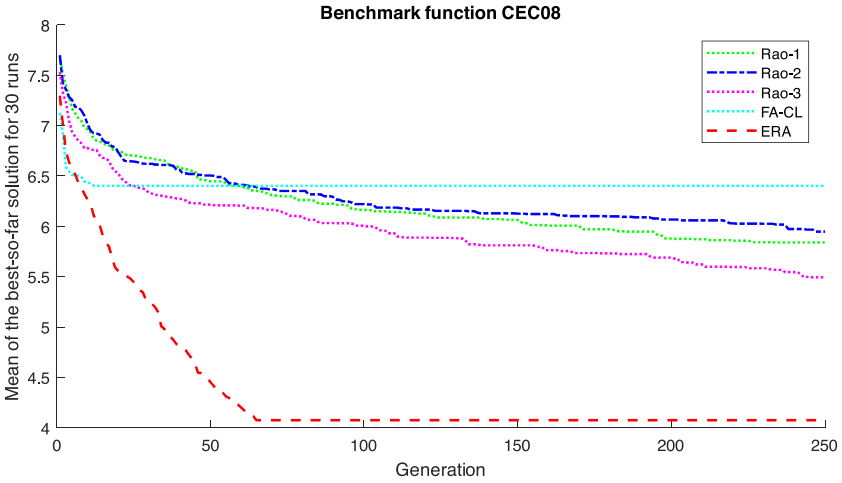

Fig. 14. Convergence analysis for CEC08.

Rao-1 with a *p*-value of bigger than 0.05. Meanwhile, for CEC04 and CEC09, ERA is much worse than Rao-1 and Rao-2 with *p*-values of less than 0.05.

Furthermore, the detailed investigations are then discussed by illustrating the convergence analysis of ERA and all the competitors. For each benchmark function, the maximum number of function evaluations is set to 30,000 with 30 runs. Fig. 12 illustrates the evolutionary processes of all algorithms until converge the optimum solution for CEC01. In this case, ERA converges to a much better solution than the other algorithms. ERA also gives similar curves for six other benchmarks:

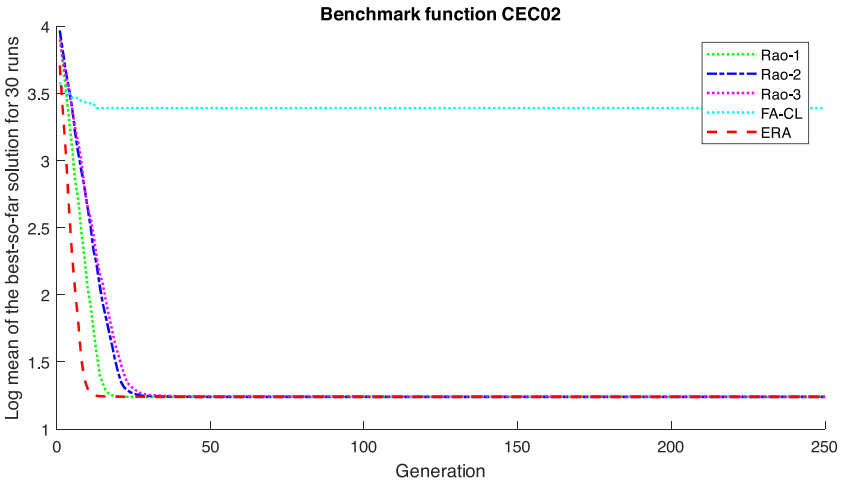

Fig. 15. Convergence analysis for CEC02.

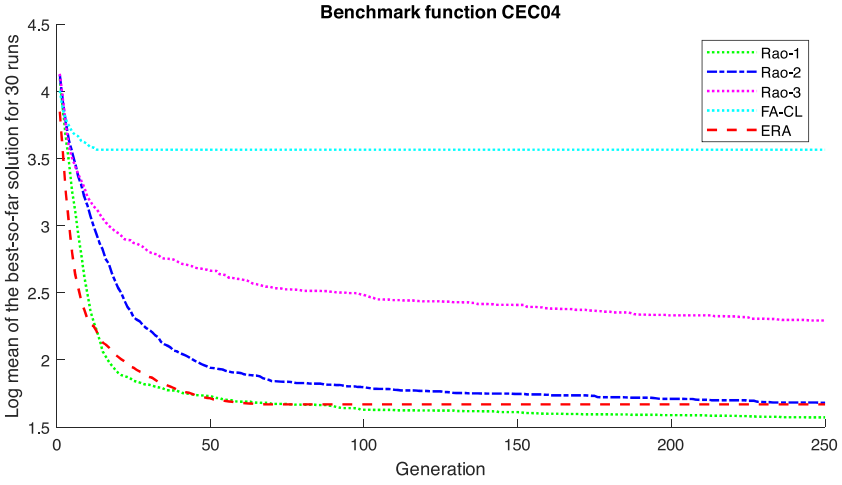

Fig. 16. Convergence analysis for CEC04.

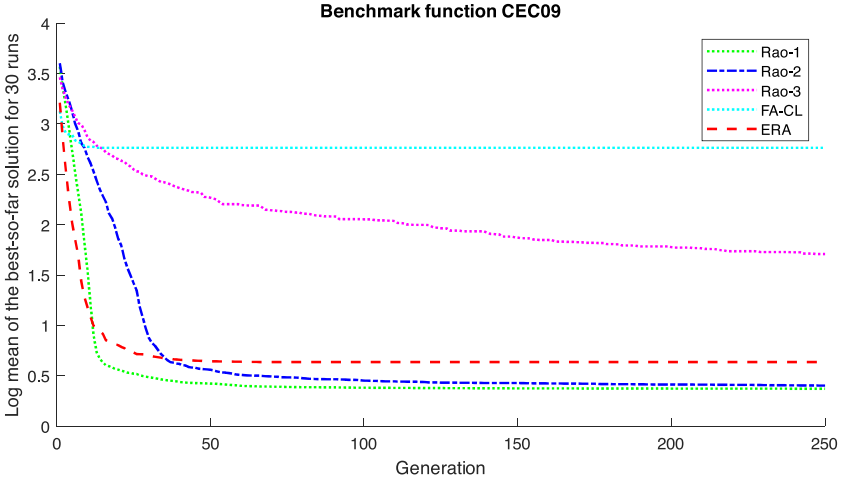

Fig. 17. Convergence analysis for CEC09.

CEC03, CEC05, CEC06, CEC07, CEC08, and CEC10. Figs. 13 and 14 illustrate the converge curves for CEC05 and CEC08. Impressively, for CEC05, ERA evolves most quickly in the beginning generations and finally gives the best mean solution of 1.152216958, which is quite close to the known global optimum of 1.

Next, the detailed investigation is then carried out for CEC02. Fig. 15 shows that ERA converges to a similar solution to Rao-1, Rao-2, and Rao-3. In addition, ERA also gives similar curves for two other benchmarks:

Table 7
Comparison of Rao-1, Rao-2, Rao-3, FA-CL, and ERA for five global trajectory optimization problems.

Problem	Metric	Rao-1	Rao-2	Rao-3	FA-CL	ERA
Cassini1	Best	5.303768392	4.936855136	5.61179549	7.074851303	5.612797557
	Worst	20.07805387	25.93297419	15.77360635	26.20831412	14.83107214
	Mean	11.87916323	12.12477947	12.56694735	16.6899857	10.61999692
	STD	3.554957586	3.64432772	2.23350672	4.840145141	2.876504936
	MFE	200000	200000	200000	200187.4333	200044.6
GTOC1	Best	631827.7829	458914.6802	376896.2971	1411461.987	710462.7745
	Worst	1548886.166	1551541.426	1536925.137	1569631.301	1311152.824
	Mean	1147746.121	1093465.404	1051211.872	1524073.714	956084.4087
	STD	233788.8767	331123.7832	266223.3551	43045.94967	136868.8532
	MFE	200000	200000	200000	200124.6333	200049.6
Messenger	Best	12.41560806	11.27514945	11.99302003	20.78291121	14.33306793
	Worst	25.50492428	20.425443	22.54997489	28.24295896	20.46142743
	Mean	18.35040915	14.97590782	16.61688953	25.51273265	16.37566883
	STD	3.328431397	2.476903152	2.802312585	2.076873921	1.412144879
	MFE	200000	200000	200000	200136.7	200047.8
Sagas	Best	76.02938156	322.8420001	246.9977338	1267.982722	504.8182077
	Worst	1615.462402	3734.488398	2310.454904	2319.048595	973.1650916
	Mean	1024.564265	1202.784813	1017.331876	1722.402349	927.9858521
	STD	345.5888343	619.2934569	310.6547919	205.0753697	99.79849535
	MFE	200000	200000	200000	200206.9	200045.6
Cassini2	Best	10.62971719	11.03729327	15.93387459	32.97381024	21.03860384
	Worst	44.68073676	36.96644582	32.11412822	47.76452256	30.01962572
	Mean	25.0919048	23.93646566	25.58562866	40.28520967	26.03675587
	STD	8.783109087	6.801655034	3.476676083	4.082917564	2.049424528
	MFE	200000	200000	200000	200088.5667	200036.6
	FMR	3.00	2.40	2.80	5.00	1.80
	Rank	4	2	3	5	1

Table 8
The *p*-values of Wilcoxon rank sum test (WRST) for five global trajectory optimization problems.

Problem	ERA vs Rao-1	ERA vs Rao-2	ERA vs Rao-3	ERA vs FA-CL
Cassini1	0.318304227	0.072445596	0.00033679	8.1975E-07
GTOC1	0.000356384	0.108689773	0.02812867	3.01986E-11
Messenger	0.005084222	0.000691252	0.437641335	3.01986E-11
Sagas	0.022360148	0.000168132	0.111986872	3.01986E-11
Cassini2	0.332854692	0.008314609	0.529782491	3.01986E-11

CEC04 and CEC09, as illustrated in Figs. 16 and 17 .

The results of FMR, WRST, and convergence curves above indicate that ERA is generally better than all the competitors in handling the effects of shift and rotation. It can be achieved since ERA is designed with two schemes: two sub-populations and evolutionary operators. Besides, it is also equipped with a fitness-based adaptation scheme to dynamically tune the three sensitive parameters: *s*, *a*, and *b* throughout the evolution process, which effectively controls the exploration and exploitation balance in searching for the global optimum solution. A detailed investigation will be provided in Section 3.6.

3.5. Evaluation on real world problems

Finally, ERA is evaluated using the global trajectory optimization problems (GTOP), which European Space Agency provides. Here, five real-world problems: Cassini1, GTOC1, Messenger, Sagas, and Cassini2 are used as the benchmarks to examine its capability to tackle the constrained problems. Here, the four cases: Cassini1, Messenger, Sagas, and Cassini2 are the minimization problems while GTOC1 is a maximization. Here, the summary of those five problems is given briefly; the more detailed descriptions and their Matlab codes can be seen in [31,33,34].

As described in [31], Cassini1 is a mission of multiple gravity assist (MGA) without the possibility of using deep space manouvres, which is related to the Cassini spacecraft trajectory design problem. The objective is to minimize the total delta velocity $\triangle V$ accumulated during the

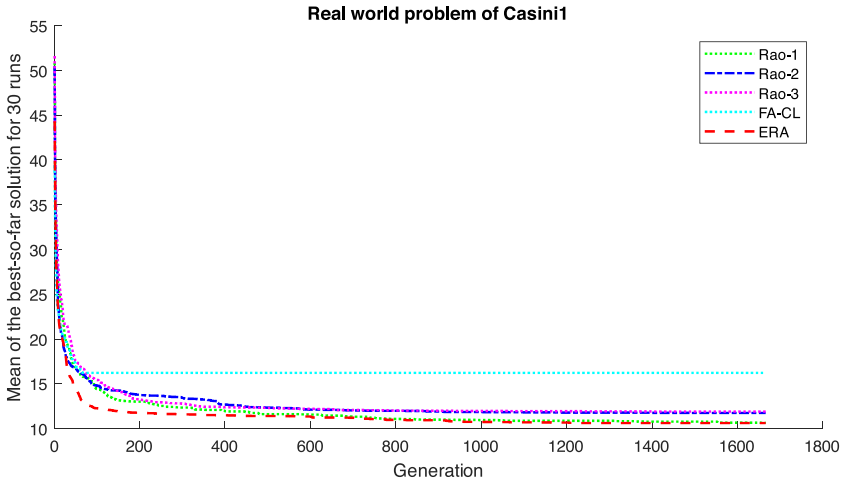

Fig. 18. Convergence analysis for Cassini1.

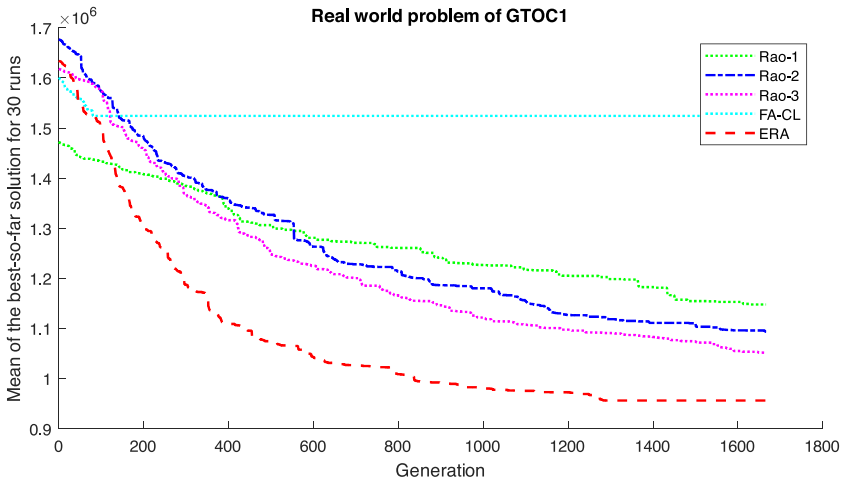

Fig. 19. Convergence analysis for GTOC1.

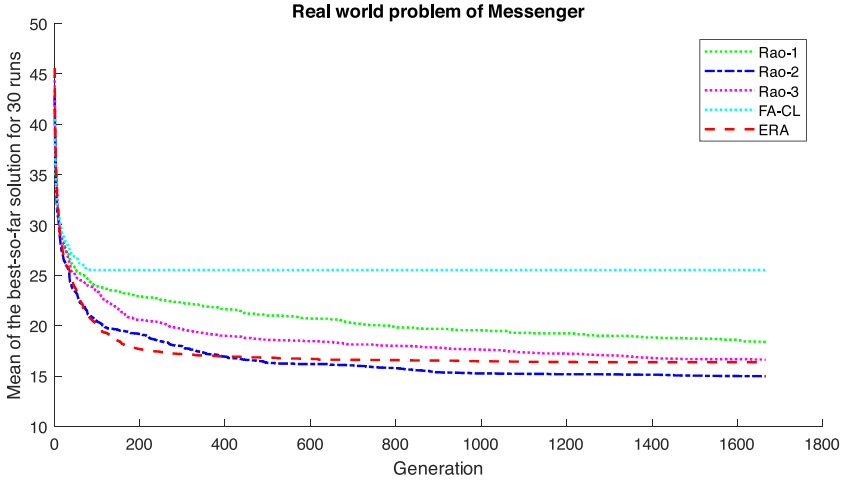

Fig. 20. Convergence analysis for Messenger.

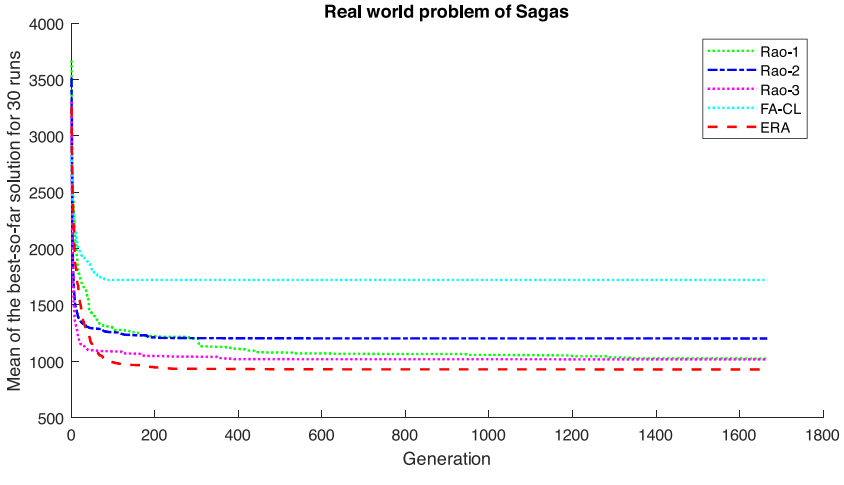

Fig. 21. Convergence analysis for Sagas.

mission with some given constraints, where the planetary fly-by sequence is Earth-Venus-Venus-Earth-Jupiter-Saturn. It has six dimensions with a known global minimum solution of 4.93 km/s.

GTOC1 is also an MGA problem, where the objective is to maximize the change in the semi-major axis of the asteroid orbit following an anaelastic impact of the spacecraft with the asteroid under several given constraints. It has 8 dimensions and the known global maximum is $f_{\max} = 1,580,599$ kg km^2/s^2. In this paper, GTOC1 is converted into a minimization problem by modifying the objective function to be $f_{\min} = 1,580,599 - f_{\max} = 0$ to make it the same as all the other problems and

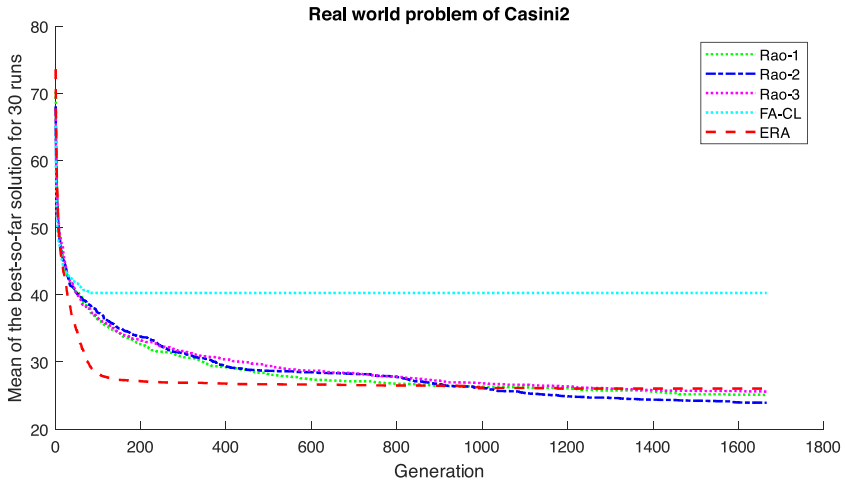

Fig. 22. Convergence analysis for Cassini2.

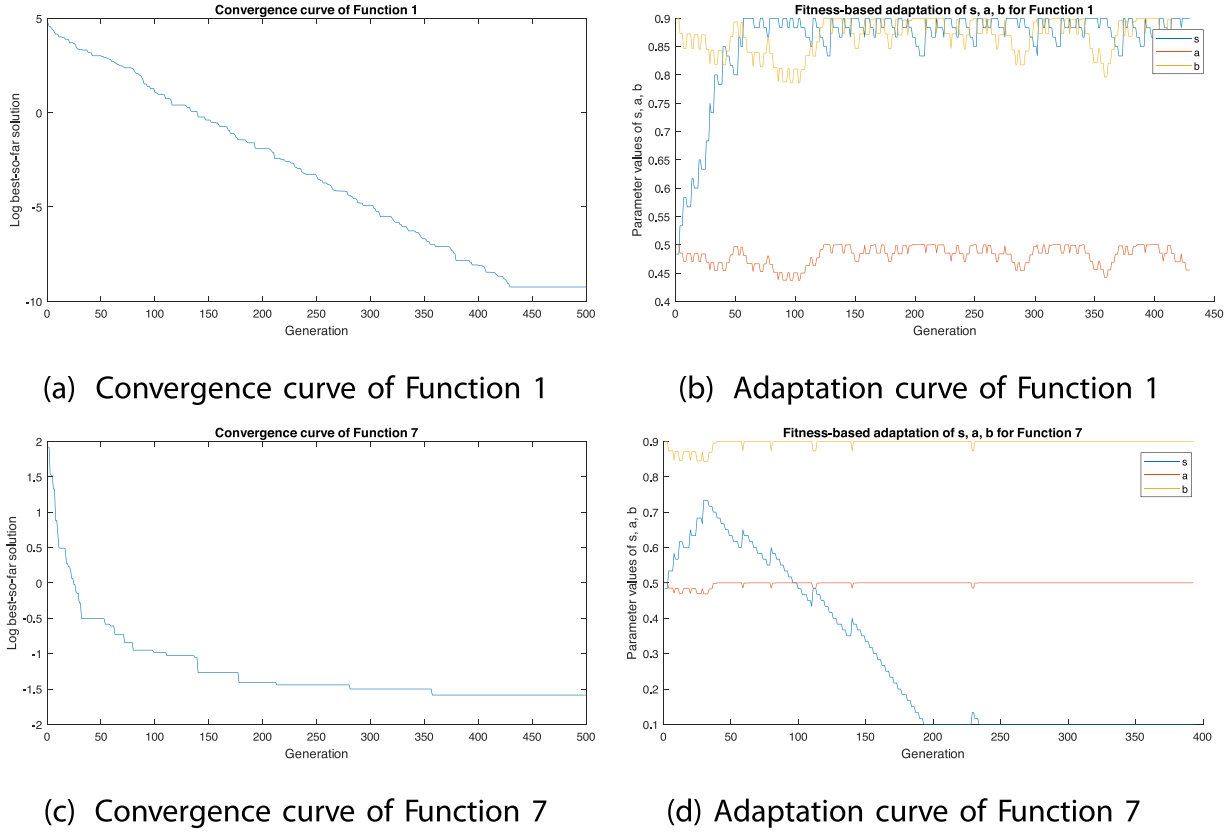

Fig. 23. Convergence and adaptation curves for 30-dimensional unimodal benchmark functions with ID = 1 and 7.

simpler in the further evaluation.

Furthermore, Messenger, Sagas, and Cassini2 are the MGA problems with the possibility of using deep space manouvres (MGA-1DSM). The objective of Messenger is to minimize the total delta velocity $\triangle V$. It has 18 dimensions, and the global minimum solution is 8.70257 km/s. Meanwhile, the objective of Sagas is to minimize the overall mission length of fly-by Jupiter and reach 50AU. It is a 12-dimensional problem with a global minimum of 18.1923 years. Finally, Cassini2 is similar to Cassini1, but it is a bigger 22-dimensional problem with much higher complexity. The known best solution is 8.92401 km/s.

In the five real-world problems, ERA is also compared with the four other algorithms in their best performances using the parameter settings described in Section 3.2. All algorithms are run 30 times with 200,000 function evaluations each as used in [31]. In addition, both FMR and WRST with the *p*-values are also provided to confirm the significance of their performance. The experimental results illustrated in Table 7 show that ERA outperforms the competitors for three out of five problems. Hence, the Friedman mean rank places ERA in the first rank with the lowest FMR of 1.80. Unfortunately, the Wilcoxon rank-sum test illustrated in Table 8 indicates that ERA significantly outperforms (with *p*-values of less than 0.05) some of the competitors. It is slightly (not significantly) better than Rao-1, Rao-2, and Rao-3 for Cassini1, GTOC1, and Sagas, respectively.

Furthermore, the detailed investigations are then discussed by

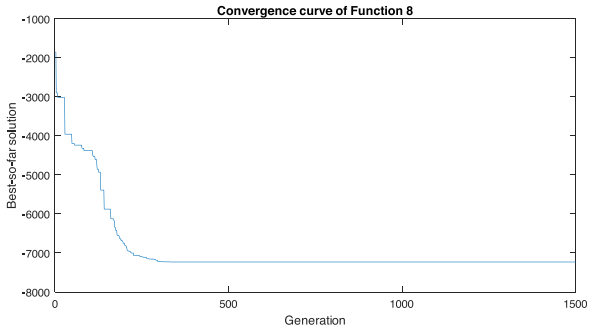

(a) Convergence curve of Function 8

(b) Adaptation curve of Function 8

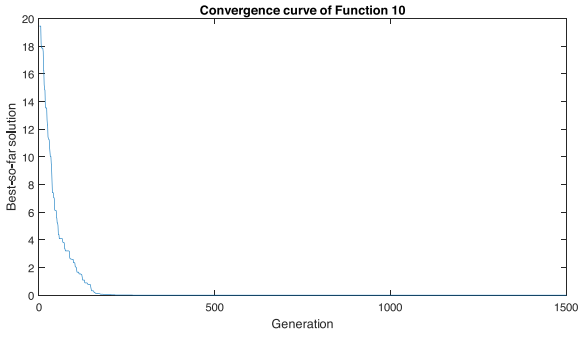

(c) Convergence curve of Function 10

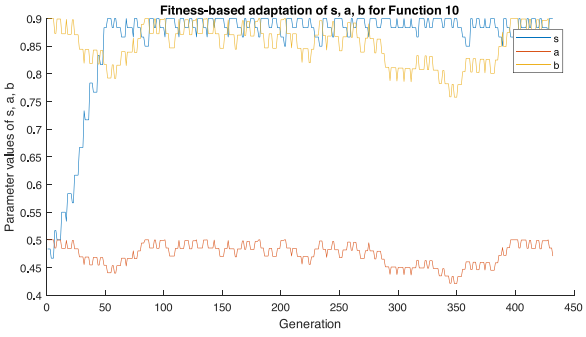

(d) Adaptation curve of Function 10

Fig. 24. Convergence and adaptation curves for 30-dimensional multimodal benchmark functions with ID = 8 and 10.

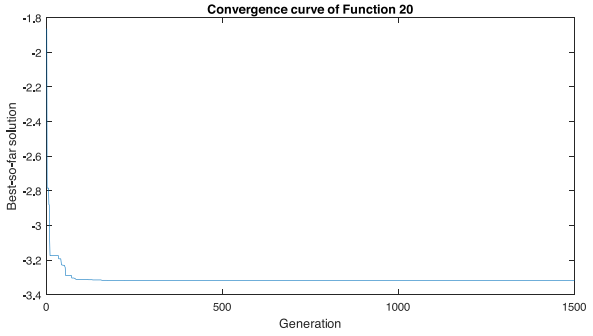

(a) Convergence curve of Function 20

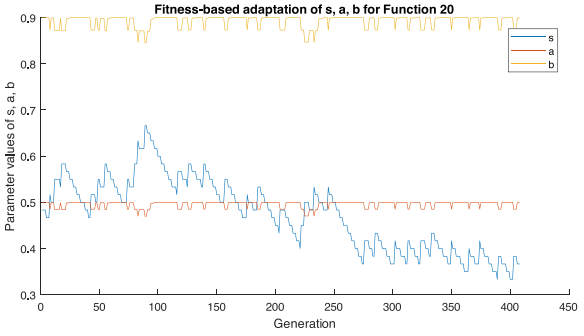

(b) Adaptation curve of Function 20

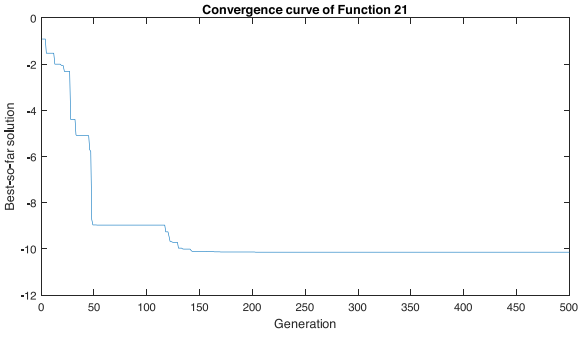

(c) Convergence curve of Function 21

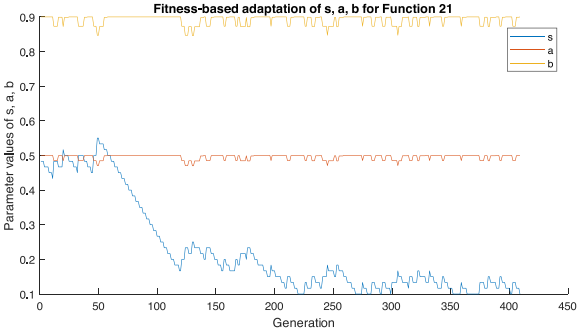

(d) Adaptation curve of Function 21

Fig. 25. Convergence and adaptation curves for low-dimensional multimodal benchmark functions with ID = 20 and 21.

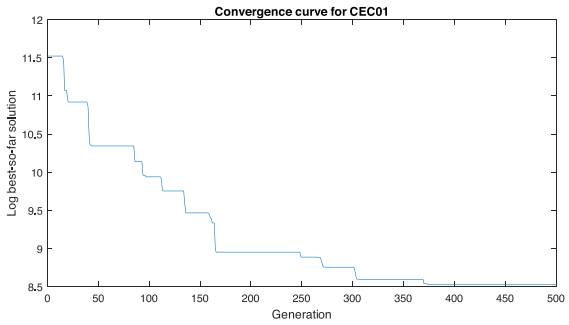

(a) Convergence curve of CEC01

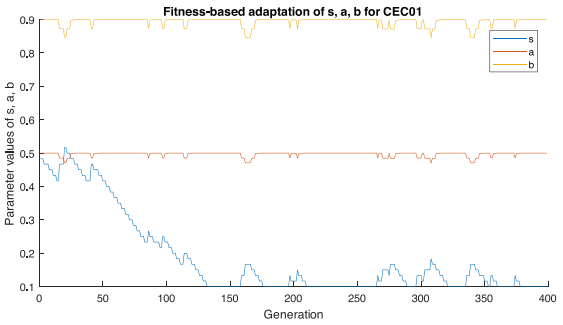

(b) Adaptation curve of CEC01

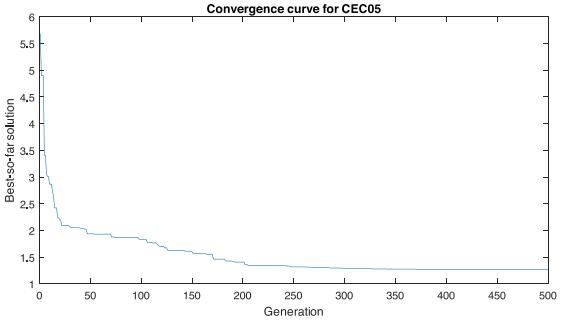

(c) Convergence curve of CEC05

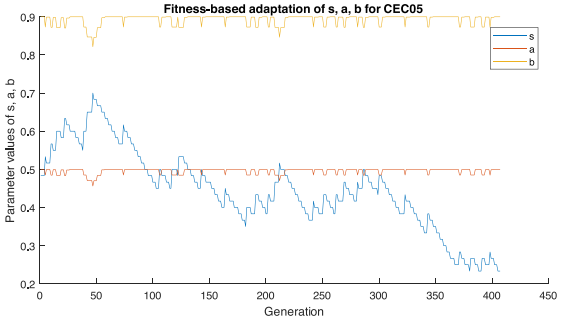

(d) Adaptation curve of CEC05

Fig. 26. Convergence and adaptation curves for CEC01 and CEC05.

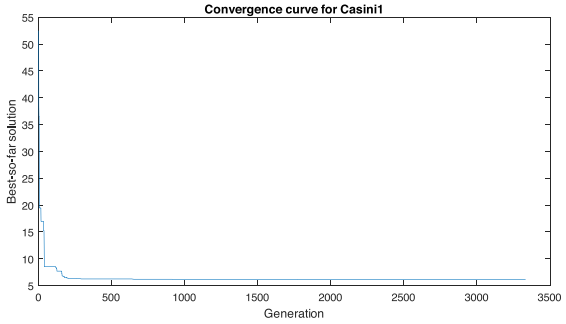

(a) Convergence curve of Cassini1

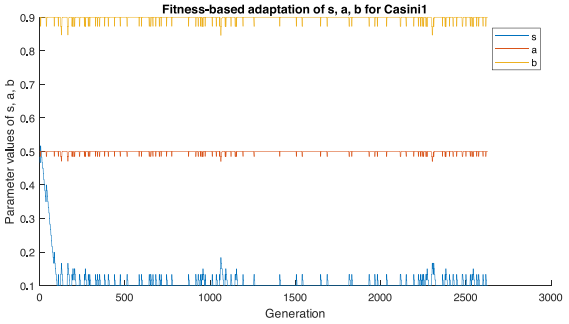

(b) Adaptation curve of Cassini1

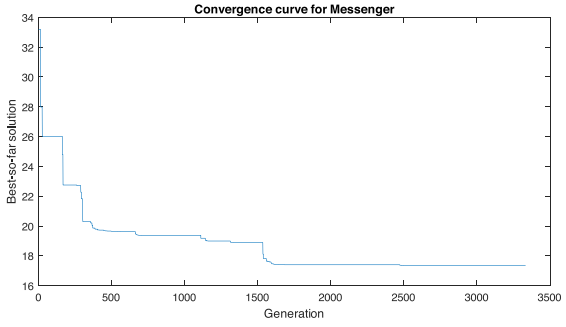

(c) Convergence curve of Messenger

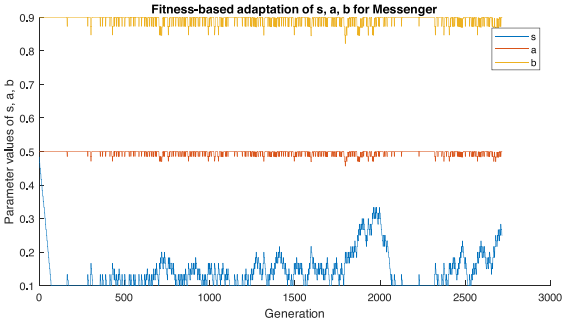

(d) Adaptation curve of Messenger

Fig. 27. Convergence and adaptation curves for the global trajectory optimization problems of Cassini1 and Messenger.

illustrating the convergence curves of ERA and the competitors. Fig. 18 illustrates the evolution of all algorithms until to the optimum solution for Cassini1. In this case, ERA converges to a better solution than the other algorithms. Like all the competitors, ERA evolves quickly in the beginning generations and gets stagnation. In addition, ERA also gives similar curves for GTOC1 and Sagas, as illustrated in Figs. 19 and 21 . However, for GTOC1, ERA reaches a much better solution.

For both Messenger and Cassini2 problems, ERA gives worse convergence curves than the Rao algorithms. Fig. 20informs that, in the beginning, ERA gives the same converge curve as the Rao-2, but it gets stuck after half of the generations while Rao-2 keeps evolving and reaches a little better solution. Meanwhile, Fig. 22 shows that ERA evolves quickly in the early generations but finally converges to a slightly worse solution than the three Rao algorithms.

However, those results of FMR, WRST, and convergence curves inform that ERA is better than the competitors in tackling the constrained real-world problems. It can be implied that the two proposed schemes: two sub-populations and evolutionary operators, as well as the introduced adaptation procedure, effectively balance the exploration and exploitation strategies. A detailed investigation regarding the adaptation scheme will be provided in Section 3.6.

3.6. Investigation on fitness-based adaptation scheme

The proposed fitness-based adaptation scheme is evaluated here using some benchmarks to see its ability to control the exploration-exploitation balance. First, two classic benchmarks (with ID = 1 and 7) are selected as the representative 30-dimensional unimodal functions. Fig. 23a illustrates that, for the Sphere function (ID = 1) that has only one global optimum, ERA converges quite fast. It can be achieved since ERA works in an exploration manner in the beginning generations and then quickly changes into an exploitation fashion, where the three parameters s, a, and b reach around the maximum values of 0.9, 0.9, and 0.5, respectively, as shown in Fig. 23b. Meanwhile, Fig. 23c illustrates that, for the Quartic function (with ID = 7) having many noises, ERA converges more slowly and gets a stagnation. In this case, ERA works in an exploration strategy throughout the evolution, where s tends to go to the minimum value of 0.1 but a and b reach the maximum values of 0.9 and 0.5, respectively, as shown in Fig. 23d.

Next, two classic benchmarks with ID = 8 and 10 are selected as the representative 30-dimensional multimodal functions. Fig. 24a illustrates that, for the Schwefel function (ID = 8) having many global optimum solutions, ERA evolves quickly in early generations but finally gets stuck on a local optimum. Here, ERA works in an exploration strategy throughout the evolution, where s tends to go around the minimum value but a and b on the maximum values, as shown in Fig. 24b. Meanwhile, Fig. 24c illustrates that, for the Ackley function (ID = 10) that also has many global optimum solutions, ERA converges quickly and also gets a stagnation. In this case, ERA tends to work in an exploitation strategy throughout the evolution, where s is on the maximum value, but a and b tends on the medium values, as shown in Fig. 24d.

Two classic benchmarks with ID = 20 and 21 are then chosen as the representative low-dimensional multimodal functions. Fig. 25a illustrates that, for the function of Hartman 6 (ID = 20) with many global optima, ERA converges quite fast to the global optimum. It can be seen that ERA works in an exploration-exploitation balance strategy throughout the evolution, where s is fluctuating between the minimum and the medium values while a and b are around the maximum values, as shown in Fig. 25b. Meanwhile, Fig. 25c illustrates that, for the function of Shekel 5 (ID = 21), ERA converges quickly to the global optimum. It tends to work in an exploration strategy throughout the evolution since Shekel 5 has a broad flat area, where s is around the minimum value, but a and b tends on the maximum values, as shown in Fig. 25d.

Two benchmarks of CEC01 and CEC05 are then chosen as the representative functions without and with both shifting and rotation, respectively. Fig. 26a illustrates that, for the function without shifting and rotation, ERA evolves slowly. Unfortunately, it gets stuck for some generations and converges to a solution far from the global optimum. It can be seen that ERA works in an exploration-exploitation balance strategy throughout the evolution, where s is fluctuating between the minimum and the medium values while a and b are around the maximum values, as shown in Fig. 26b. Meanwhile, Fig. 26c illustrates that, for the shifted and rotated function, ERA converges quickly to a solution near the global optimum of 1. It works dynamically in exploration and exploitation strategy during the evolution, where s is around the medium value, but a and b tends on the maximum values, as shown in Fig. 26d.

Finally, both Cassini1 and Messenger are selected as the representative of the real-world problems. Fig. 27a illustrates that ERA evolves quickly in the beginning generations, but it gets stuck and converges to a solution far from the global optimum. It can be seen that ERA tends to work in an exploration manner throughout the evolution, where s is on the minimum value while a and b are around the maximum values, as shown in Fig. 27b. Meanwhile, Fig. 27c shows that ERA evolves slowly and converges to a solution near the global optimum. It works dynamically in exploration and exploitation strategy during the evolution, where s is fluctuating between the minimum and the medium values, but a and b tends on the maximum values, as shown in Fig. 27d.

The convergence and adaptation curves above prove that the proposed adaptation scheme effectively controls the exploration and exploitation balance. This scheme makes ERA can handle many types of benchmark functions: unimodal, multimodal, shifted, rotated, and also real-world problems.

4. Conclusions

The proposed evolutionary Rao algorithm (ERA) works very well based on two additional schemes: splitting the population into two subpopulations based on their qualities: high and low, with a proper portion adaptively during the evolution, and exploiting two evolutionary operators: crossover and mutation. The evaluations of twenty-three classic benchmark functions and ten CEC-C06 2019 benchmarks show that it significantly outperforms all the competitors: Rao-1, Rao-2, Rao-3, and FA-CL, where it reaches the Friedman mean rank of 1.52 and 1.50, respectively, with the p-values of Wilcoxon rank-sum test of less than 0.05 for most of the benchmarks. Examining the five real-world global trajectory optimization problems inform that ERA gives significant performances only for some of the competitors. Detailed investigations prove that all the proposed schemes work well as they are designed and make ERA effectively control the exploration and exploitation balance. All the proposed schemes make ERA able to handle most of the benchmark functions with various types: unimodal, multimodal, shifted, rotated, and also real-world problems. However, in the future, a new advanced adaptation scheme to update the population size dynamically throughout the evolutionary process as well as a better mutation scheme will be created to improve the performance of ERA. Besides, it will be comprehensively examined using more challenging benchmarks.

Declaration of Competing Interest

The authors report no declarations of interest.

References

[1] K. Hussain, M.N. Mohd Salleh, S. Cheng, Y. Shi, Metaheuristic research: a comprehensive survey, Artif. Intel. Rev. 52 (4) (2019) 2191–2233, https://doi.org/10.1007/s10462-017-9605-z.

[2] J.H. Holland, Genetic algorithms, Sci. Am. 267 (1) (1992) 66–72, https://doi.org/10.1038/scientificamerican0792-66.

[3] A. Lambora, K. Gupta, K. Chopra, Genetic Algorithm- A Literature Review, in: in: 2019 International Conference on Machine Learning, Big Data, Cloud and Parallel Computing (COMITCon). doi:10.1109/COMITCon.2019.8862255, 2019, pp. 380–384.
[4] F. Murillo, T. Neuenschwander, R. Dornberger, T. Hanne, Optimization of a Robotic Manipulation Path by an Evolution Strategy and Particle Swarm Optimization, in: in: ACM International Conference Proceeding Series, Association for Computing Machinery. doi:10.1145/3396474.3396488, 2020, pp. 36–41.
[5] Z. Li, Q. Zhang, Variable metric evolution strategies by mutation matrix adaptation, Inform. Sci. 541 (2020) 136–151, https://doi.org/10.1016/j.ins.2020.05.091.
[6] J. Cheng, Z. Pan, H. Liang, Z. Gao, J. Gao, Differential evolution algorithm with fitness and diversity ranking-based mutation operator, Swarm and Evolutionary Computation 61 (2021) 100816, https://doi.org/10.1016/j.swevo.2020.100816.
[7] R. Zhang, Z. Qiu, Optimizing hyper-parameters of neural networks with swarm intelligence: A novel framework for credit scoring, PLoS ONE 15 (6). doi:10.1371/journal.pone.0234254.
[8] V. Mp, B. Anand, Microprocessors and Microsystems Particle swarm optimization technique for multilevel inverters in solar harvesting micro grid system, Microprocess. Microsyst. 79 (2020) 103288, https://doi.org/10.1016/j.micpro.2020.103288.
[9] D. Kumar, B.G.R. Gandhi, R.K. Bhattacharjya, Firefly algorithm and its applications in engineering optimization, Model. Optimiz. Sci. Technol. 16 (2020) 93–103, https://doi.org/10.1007/978-3-030-26458-1_6.
[10] V. Kumar, D. Kumar, A Systematic Review on Firefly Algorithm: Past, Present, and Future, Archives of Computational Methods in Engineeringdoi:10.1007/s11831-020-09498-y. URL https://www.x-mol.com/paper/1311351373626052608.
[11] S. Gupta, K. Deep, Enhanced leadership-inspired grey wolf optimizer for global optimization problems, Eng. Comput. 36 (4) (2020) 1777–1800, https://doi.org/10.1007/s00366-019-00795-0.
[12] J. C. Bansal, S. Singh, A better exploration strategy in Grey Wolf Optimizer, Journal of Ambient Intelligence and Humanized Computingdoi:10.1007/s12652-020-02153-1.
[13] A.S. Assiri, A.G. Hussien, M. Amin, Ant lion optimization: variants, hybrids, and applications, IEEE Access 8 (2020) 77746–77764, https://doi.org/10.1109/ACCESS.2020.2990338.
[14] J.H. Holland, J.H. Holland, Others, Adaptation in natural and artificial systems: an introductory analysis with applications to biology, control, and artificial intelligence, University of Michigan press, 1975.
[15] A.C. Rizal, S. Suyanto, Human-Like Constrained-Mating to Make Genetic Algorithm More Explorative, in: in: 2020 8th International Conference on Information and Communication Technology (ICoICT), IEEE, doi:https://doi.org/10.1109/ICoICT49345.2020.9166387. URL https://ieeexplore.ieee.org/document/9166387/, 2020, pp. 1–5.
[16] J. Kennedy, R. Eberhart, Particle swarm optimization, in: Proceedings of ICNN'95 - International Conference on Neural Networks, Vol. 4 (1995) 1942–1948.
[17] D. Li, W. Guo, A. Lerch, Y. Li, L. Wang, Q. Wu, An adaptive particle swarm optimizer with decoupled exploration and exploitation for large scale optimization, Swarm and Evolutionary Computation 60 (2021) 100789, https://doi.org/10.1016/j.swevo.2020.100789.
[18] D. Sedighizadeh, E. Masehian, M. Sedighizadeh, H. Akbaripour, GEPSO: A new generalized particle swarm optimization algorithm, Math. Comput. Simul. 179 (2021) 194–212, https://doi.org/10.1016/j.matcom.2020.08.013.
[19] X.-S. Yang, Firefly algorithms for multimodal optimization, in: Stochastic Algorithms: Foundations and Applications, Springer Berlin Heidelberg, 2009, pp. 169–178.
[20] I. Fister, I. Fister, X.-S. Yang, J. Brest, A comprehensive review of firefly algorithms, Swarm Evolut. Comput. 13 (2013) 34–46.
[21] H. Peng, W. Zhu, C. Deng, Z. Wu, Enhancing firefly algorithm with courtship learning, Inform. Sci. 543 (2020) 18–42, https://doi.org/10.1016/j.ins.2020.05.111.
[22] S. Wu, Z. Wu, H. Peng, Enhancing Firefly Algorithm with Best Neighbor Guided Search Strategy, Wuhan Univ. J. Natural Sci. 24 (6) (2019) 524–536, https://doi.org/10.1007/s11859-019-1432-4.
[23] S. Mirjalili, S.M. Mirjalili, A. Lewis, Grey Wolf Optimizer, Adv. Eng. Softw. 69 (2014) 46–61, https://doi.org/10.1016/j.advengsoft.2013.12.007.
[24] J. Luo, Z. Liu, Novel grey wolf optimization based on modified differential evolution for numerical function optimization, Appl. Intel. 50 (2) (2020) 468–486, https://doi.org/10.1007/s10489-019-01521-5.
[25] S. Bahuguna, A. Pal, Annealed grey wolf optimization, Adv. Math.: Sci. J. 9 (8) (2020) 5477–5489, https://doi.org/10.37418/amsj.9.8.18.
[26] W. Long, T. Wu, S. Cai, X. Liang, J. Jiao, M. Xu, A Novel Grey Wolf Optimizer Algorithm with Refraction Learning, IEEE Access 7 (2019) 57805–57819, https://doi.org/10.1109/ACCESS.2019.2910813.
[27] M. H. Nadimi-Shahraki, S. Taghian, S. Mirjalili, An improved grey wolf optimizer for solving engineering problems, Expert Systems with Applications 166. doi:10.1016/j.eswa.2020.113917. URL https://www.sciencedirect.com/science/article/pii/S0957417420307107.
[28] S. Mirjalili, The ant lion optimizer, Adv. Eng. Softw. 83 (2015) 80–98, https://doi.org/10.1016/j.advengsoft.2015.01.010.
[29] R.V. Rao, Rao algorithms: Three metaphor-less simple algorithms for solving optimization problems, Int. J. Ind. Eng. Comput. 11 (1) (2020) 107–130, doi:10.5267/j.ijiec.2019.6.002.
[30] J.M. Abdullah, Fitness dependent optimizer: inspired by the bee swarming reproductive process, IEEE Access 7 (2019) 43473–43486, https://doi.org/10.1109/ACCESS.2019.2907012.
[31] T. Vinko, D. Izzo, Global Optimisation Heuristics and Test Problems for Preliminary Spacecraft Trajectory Design, Tech. Rep. GOHTPPSTD, 2008. URL http://www.esa.int/gsp/ACT/doc/INF/pub/ACT-TNT-INF-2008-GOHTPPSTD.pdf.
[32] X. Xia, L. Gui, Y. Zhang, X. Xu, F. Yu, A fitness-based adaptive differential evolution algorithm, Inform. Sci. 549 (2021) 116–141, https://doi.org/10.1016/j.ins.2020.11.015.
[33] E. S. A. Advanced Concepts Team, Global Trajectory Optimisation Problems Database (2021). URL https://www.esa.int/gsp/ACT/projects/gtop/.
[34] T. Vinko, D. Izzo, C. Bombardelli, Benchmarking different global optimisation techniques for preliminary spacetrajectory design, in: in: 58th International Astronautical Congress, URL http://www.esa.int/gsp/ACT/doc/MAD/pub/ACT-RPR-MAD-2007-BenchmarkingDifferentGlobalOptimisationTechniques.pdf, 2007.

Suyanto Suyanto received the B.Sc. on Informatics Engineering from STT Telkom (now Telkom University), Bandung, Indonesia in 1998, the M.Sc. on Complex Adaptive Systems from Chalmers University of Technology, Goteborg, Sweden, in 2006, and the Doctor on Computer Science from Universitas Gadjah Mada in 2016. Since 2000, he joined STT Telkom as a lecturer in School of Computing. His research interests include artificial intelligence, machine learning, deep learning, swarm intelligence, speech processing, and computational linguistics. Scopus ID: 56843751100, Researcher ID: AAB-5223-2021, Publon ID: 4171399, Orcid: https://orcid.org/0000-0002-8897-8091.

Agung Toto Wibowo received the B.Sc. on Informatics Engineering from STT Telkom (now Telkom University), Bandung, Indonesia in 2005, the M.T. on Electrical Engineering from Bandung Institute of Technology, Indonesia, in 2009, and the Doctor of Philosophy on Computing Science from University of Aberdeen in 2019. Since 2006, he joined IT Telkom as a lecturer in School of Computing. His research interests include artificial intelligence, machine learning, deep learning, swarm intelligence, speech processing, and recommender systems. Scopus ID: 57195616672

Said Al Faraby received M.Sc. in Artificial Intelligence from University of Amsterdam in 2015. Before that, he completed B. Sc. on Informatics Engineering from IT Telkom (now Telkom University), Bandung, Indonesia in 2010. Since 2015 he joined Telkom University as a lecturer at School of Computing. His research interests mainly in the area of machine learning, natural language processing, and intelligence systems. Scopus ID: 55845346500, Publon ID: 4214736.

Siti Saadah received the Bachelor and Master degree in Informatics Engineering from Telkom Institute of Technology (now Telkom University), Bandung, Indonesia in 2009 and 2012. Since 2009, she joined Telkom University as a lecturer in School of Computing. She is Teaching Design and Analysis Algorithm, Artificial Intelligence, Theory Authomata at Telkom University. Her research interests include machine learning, financial computing, AI healthcare, prediction and simulation. Scopus ID: 55523371300, Researcher ID: AAD-6187-2021, Publon ID: 4215578.

Rita Rismala received the Bachelor and Master degree in Informatics Engineering from Telkom Institute of Technology (now Telkom University), Bandung, Indonesia in 2010 and 2013. She is now a Ph.D student in School of Electrical Engineering and Informatics, Bandung Institute of Technology, Bandung, Indonesia. Since 2011, she joined Telkom University as a lecturer in School of Computing. Her research interests include machine learning, deep learning, recommender system, and natural language processing. Scopus ID: 55844928300, Researcher ID: AAE-4960-2021, Publon ID: 4187049.